科学通报 2018 Vol. 63 No. 18: 1783 ~ 1802

Comments

Science in China
SCIENCE CHINA PRESS

Research progress of photodynamic reactive oxygen species

Jiang Xinpeng, Dai Zhifei*

Department of Biomedical Engineering, College of Engineering, Peking University, Beijing 100871, China * Contact, E-mail: zhifei.dai@pku.edu.cn

Received 2018-03-08, revised 2018-04-19, accepted 2018-05-22, published online 2018-06-14 Supported by the National Major Scientific Research Instrument Development Project (81727803) and the National Key R&D Program of Nanotechnology (2016YFA0201400)

Abstract In the process of photodynamic therapy (PDT) for cancer treatment, reactive oxygen species (ROS) mediated by photosensitizers play a key role. This article mainly introduces the methods of increasing reactive oxygen species (ROS) at the target site from the aspects of photosensitizer targeting, light frequency conversion, and oxygen delivery involved in the three elements of PDT (light, oxygen, and photosensitizer); summarizes the photomultiplier tubes, single-photon avalanche diodes, and negative feedback avalanche diode detectors for direct detection of singlet oxygen, as well as new fluorescent or chemical probes for indirect detection of singlet oxygen, hydroxyl or superoxide anions; describes the apoptotic signaling pathways triggered by ROS from the gene, protein to the cell level, and the mechanism of action of immune response inducing tumor cell apoptosis.

Keywords: photodynamic therapy, reactive oxygen species, singlet oxygen, photosensitizer, detection, mechanism of action

Cancer is a very serious medical and social problem. Cancer is the second leading cause of death in the world. According to statistics from the World Health Organization (WHO), cancer caused 8.8 million deaths in 2015. From a global perspective, nearly 1/6 of deaths are caused by cancer. Therefore, anti-cancer treatment is particularly important in improving human health. Traditional tumor treatment methods include surgery, radiotherapy, and chemotherapy. These treatment methods have great trauma or toxic side effects on patients, and often have poor treatment effects. Photodynamic therapy (PDT) is an emerging tumor treatment method. Its basic principle is: a light source of a certain frequency (generally the excitation light source of the photosensitizer) is used to irradiate the tumor site where the photosensitizer is enriched. After absorbing light, the photosensitizer transitions to an excited state and then interacts with surrounding biological molecules or oxygen to produce reactive oxygen species (ROS). ROS kills tumor cells and achieves the purpose of treating tumors [1]. When PDT is used to treat tumors, the dual targeting of photosensitizer and light can improve its treatment effect. As a key substance for killing tumor cells in PDT, the production and content detection of ROS is very important. Currently, a variety of photosensitizers and ROS detection technologies are under research. In addition, the anti-tumor mechanism of ROS is also extremely complex, involving multiple biochemical pathways and immune responses. The following will focus on the generation of ROS and its influencing factors, ROS detection technology, and the role of ROS. Use mechanism.

1 Basic properties of active oxygen

ROS mainly include singlet oxygen ($^1O_2$), hydrogen peroxide (H_2O_2), hydroxy (·OH), superoxide anion radical ($O_2\cdot^-$), nitric oxide (NO) (NO), hypochlorite (ClO^-), peroxynitrite ($ONOO\cdot^-$), etc. Reactive oxygen species can rapidly oxidize reducing substances in the body, such as unsaturated lipids. Except for H_2O_2 and NO, other reactive oxygen species have a short lifespan. $^1O_2$ The lifetime of $^1O_2$ in H_2O is 2~3.5 μs [2], while the lifetime of $^1O_2$ in cells is even shorter, ranging from 100 ns in the lipid region of the cell membrane to 250 ns in the cytoplasm. The diffusion distance of singlet oxygen in the cell environment is only 45 nm, so it cannot pass through the monolayer cell membrane [3,4]. The lifetimes of singlet oxygen in different solvents are shown in Table 1 [3]. The half-life of ·OH is only 1 ns, and it is also the most active ROS [5]. ·OH is considered to be a highly reactive oxygen species (hROS) because of its strong oxidizing properties and the fact that this compound can directly oxidize nucleic acids, proteins and lipids [6]. The half-life of $O_2\cdot^-$ is from 5 s to several hundred seconds [7]. It is also a precursor of H_2O_2 and ·OH [8]. $^1O_2$ is considered to be one of the most destructive ROS [9] and one of the most important ROS in PDT. It can release ions when it decays to ground state oxygen in its natural state.

Citation format: Jiang Xinpeng, Dai Zhifei. Research progress of photodynamic reactive oxygen species. Chinese Science Bulletin, 2018, 63: 1783–1802
Jiang X P, Dai Z F. Reactive oxygen species in photodynamic therapy (in Chinese). Chin Sci Bull, 2018, 63: 1783–1802, doi: 10.1360/N972018-00214

Table **1** Lifetime of singlet oxygen in different solvents [3]

Table 1 Lifetime of singlet oxygen in different solvents[3]

Solvent	Singlet oxygen lifetime (ÿs)
	3.5
H2OMethanol	10
Pyridine	33
CF3Cl	1000
Chloroform	300
CS2	1470
Cyclohexane	23
CD3OD	227
C6D6	3900
D2O	68

The singlet oxygen can be directly detected by emitting fluorescence at 1270 nm.

The specific detection method is as follows .

quenched by special quenchers, such as sodium azide (SA, a quencher of singlet oxygen

quencher) and D-mannitol (DM, a hydroxyl quencher).

2 Generation of reactive oxygen species

2.1 Generation and clearance of endogenous ROS

Under normal circumstances, about 90% of the reactive oxygen species in the body are generated by mitochondrial electrons.

Transfer chain (mitochondrial electron transfer chain, mitETC)

[10] The yield of ROS produced by ETC varies with cell hypoxia, light stimulation,

The oxygen content of oxygen in the mitochondria increases with stress, oxygen reperfusion, aging, and mitochondrial

respiratory inhibition [11]. More than 90% of oxygen is reduced to oxygen by cytochrome oxidase in the mitochondria.

into water molecules, only a small part of which is converted into partially reduced products, i.e., active

Active oxygen (such as superoxide, hydroxide, hydroxyl radical).

The production of reactive oxygen species and the conversion of different reactive oxygen species

into each other[12], such as O2 ·ÿ, which can be converted into H2O2 by endogenous superoxide

dismutase (SOD). Granulocytes and macrophages also produce a large amount of ROS[9], which can also

It is induced by stress factors such as tumor necrosis factor ÿ (TNF-ÿ).

There are many endogenous photosensitizers in the body.

The main photosensitizing substances are flavin, porphyrin,

Rhodopsin, quinone compounds, etc. [9]. Tumor cells express flavins in large quantities

Riboflavin carrier protein (RCP)[13]

The flavin content in tumor cells is relatively high. Riboflavin-5-phosphate (FAD) and

Flavin adenine dinucleotide (FMN) is an endogenous photosensitizer.

The blue light can stimulate the mitochondria to the maximum extent and produce ROS.

It is shown [14] that under normal light, it has no toxic effect on the human body.

The body also produces singlet oxygen independently of light.

It depends on the respiratory burst of macrophages, in which NADPH is oxidized

Enzymes produce O2 ·ÿ, which spontaneously or enzymatically decomposes into H2O2, which is then

catalytically reduced to hypochlorous acid (HOCl). Finally, H2O2 and HOCl react spontaneously .

The reaction generates 1 O2 [9].

The removal of reactive oxygen species depends on the active oxygen scavenging enzymes in the body and

Non-enzymatic antioxidant molecules. Active oxygen scavenging enzymes mainly include peroxidase

and superoxide dismutase (SOD)[15], where SOD has different metal chelates

Combined forms, such as Cu-, Zn-, Mn-SOD, among which the role of Mn-SOD

The strongest [16]. The non-enzymatic antioxidant molecules of cells are uric acid, ascorbic acid,

ÿ-Tocopherol and sulfhydryl-containing molecules such as glutathione (GSH), cysteine

Acid (Cys), etc.[17].

2.2 Photosensitizer

Photosensitizer (PS) is a type of photosensitive

The photon is long and it jumps from the ground state to the excited state, and then the absorbed energy

transfer to nearby oxygen molecules to produce singlet oxygen, or

The substances undergo photochemical reactions to produce photosensitizers of active oxygen free radicals.

Commonly used

photosensitizers are: Porphyrin-based photosensitizers include porphyrin,

Phthalocyanines, chlorins, bacteriochlorins, and rhodocyanines; non-porphyrin-based photocatalysts

Sensitizers include psoralens, anthraquinones such as hypericin and hypocrellin,

Cyanines, phenothiazinium compounds such as methylene blue, Nile blue analogs,

Aniline blue, rhodamine, triarylmethane and acridine etc.[18].

Sensitizers such as hematoporphyrin ether and photoporphyrin[3] have short excitation wavelengths and are

The retention time in the body is long, which brings great inconvenience to patients.

Compared with the first generation of photosensitizers, the sensitizers have been improved and even have targeted

[19]. Most second-generation photosensitizers are also based on porphyrin structures, such as

Such as benzoporphyrin, rhodocyanine, texaphyrin, phthalocyanine, naphthalocyanine and

Protoporphyrin IX (PpIX)[20~22].

2.3 ROS generation mechanism

There are two mechanisms for the generation of exogenous ROS:

Energy transfer or energy transfer. Energy transfer mainly produces singlet oxygen, while electron

transfer produces other

Reactive oxygen free radicals, in PDT, are called type II PDT and type I PDT

PDT. The mechanism of singlet oxygen generation is shown in Figure 1:

Under the irradiation, the photosensitizer is excited and then transitions back to the ground state, and

The energy is transferred to the oxygen molecule, and the oxygen molecule is excited from the triplet state after receiving the energy.

To the singlet state. Singlet oxygen has two forms but both end up as

O2(a1 ÿg)[18]. The concentration of singlet oxygen and other factors

The relationship is as follows[23]:

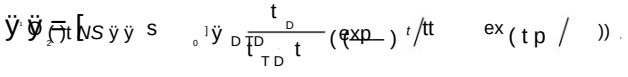

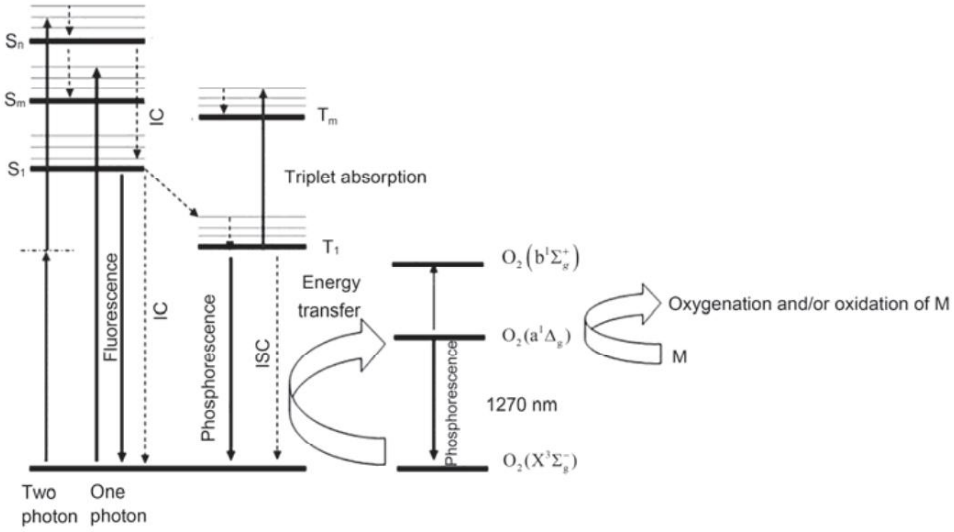

Figure **1** Mechanism of singlet oxygen generation[18]

Figure 1 The mechanism of singlet oxygen generation[18]

Where [1 O2] is the singlet oxygen concentration at time t, N is the excitation pulse is the number of photons, ÿ is the photosensitizer absorption cross section, S0 is the photosensitizer $ÿ_D$ concentration, is the singlet oxygen quantum yield, T is the photosensitizer triplet lifetime, and D is t Singlet oxygen lifetime.

2.4 Factors affecting ROS production and corresponding photosensitizers

Since photosensitizer, light and oxygen are the three elements of PDT, Factors related to these three elements can affect the generation of ROS. The factors that affect the efficacy of PDT include the target of the photosensitizer Tropism, ROS production, water solubility, dark toxicity, and local oxygen in tumors Concentration, illumination frequency, temperature, self-quenching of singlet oxygen, etc. **2.4.1** Targeting of photosensitizers

Targeted photosensitizers can accumulate in tumor sites and improve Local photosensitizer concentration and PDT efficacy and reduction of toxic side effects. Research This indicates that a very small amount of ROS in mitochondria can generate a larger amount of ROS than in the nucleus. In low-dose PDT, the ROS produced by mitochondria ROS produced by the respiratory transport chain plays a major role in cell apoptosis. As the PDT dose increases, the effect of endogenous reactive oxygen species becomes It is not obvious[25], so targeting photosensitizers to mitochondria is an important way to improve PDT The localization of photosensitizers in different organelles will Causes different cell death mechanisms. Studies have shown that [22], when photosensitizer When the cells are mainly concentrated in mitochondria and lysosomes, the cell death pathway is mainly is apoptosis; when photosensitizers accumulate in the endoplasmic reticulum or cell membrane, cells die The apoptosis pathways are autophagy and direct

death. Triphenylphosphine[26] has mitochondrial targeting, and Tang's group[27] Linking triphenylphosphine to a photosensitizer enables targeting to mitochondria for selective Selectively triggering local ROS burst in mitochondria and initiating mitochondrial intrinsic apoptosis The Chen group[28] synthesized a phthalocyanine photosensitizer linked to folic acid . The study showed that it has both mitochondrial and endoplasmic reticulum targeting properties.

Because tumors have an acidic environment, the pH inside tumor cells is usually 0.2~1 lower than normal cells, so pH-sensitive Aoki's research topic The group[29,30] designed a pH-sensitive cyclometallated Ir(III) complex for photosensitization Agent, containing 2-(5ÿ-N,N-diethylamino-4ÿ-tolyl)pyridine ligand The structure is shown in Figure 2. The complex is in a neutral and slightly acidic environment. The luminescence microscopy study of HeLa-S3 cells showed that it can be used for selective staining. Lysosomes are acidic organelles in cells. In addition, Jeong's group[31] reported a pH-sensitive MPEG poly(ÿ-amino ester) polymer micelles (Figure 3)

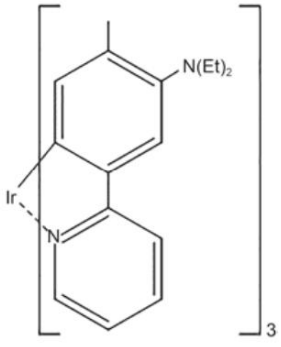

Figure **2** pH-sensitive cyclometallated iridium complex photosensitizer[29,30]

Figure 2 A pH sensitive ring metal Iridium complex photosensitiz-er[29,30]

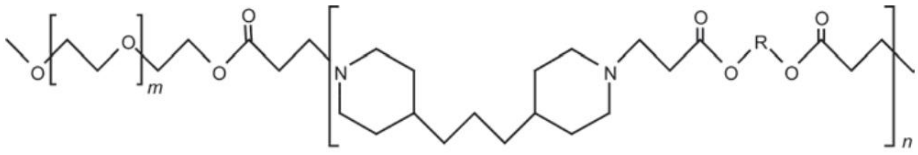

Figure **3** pH-sensitive polymer micelles[31]

Figure 3 A pH sensitive polymer micelle[31]

The micelles showed strong pH-dependent micellar disaggregation at the acidic extracellular pH of tumors because the tertiary amine groups (pKb = 6.5) in the hydrophobic aminoester block were protonated under acidic conditions below pH 6.5.

In addition, linking photosensitizers with targeted antibodies or peptides, or targeted biological small molecules can improve the PDT effect. For example, near-infrared phthalocyanine blue photosensitizer IR700 is combined with a monoclonal antibody targeting epidermal growth factor [32], and porphyrin photosensitizers combined with IgG antibodies have human epidermal growth factor receptor 2 (HER2) targeting [33]. Tsai's group [34] used heparin, phospholipids and histidine as carriers of photosensitizers to synthesize a pH-sensitive micelle, and effectively prevented the aggregation of photosensitizers. Varchi's group [35] linked photosensitizers to non-steroidal anti-androgen molecules for the treatment of prostate cancer. Ouk's group [36] synthesized a new compound composed of a derivative of polymyxin B covalently linked to a cationic porphyrin, and this compound has enhanced activity and targeting properties. Sulfonated polyethylene ether imine can also be combined with photosensitizers for targeting to selectins, membrane adhesion proteins, etc. [37]. There are also non-infectious viruses used as targeting carriers such as Steinmetz's group [38] used natural non-infectious nanoparticles of cowpea mosaic virus (CPMV) to improve melanoma treatment. **2.4.2** Oxygen concentration Due to the

generation of ROS, especially singlet oxygen, a large amount of oxygen is required. However, tumor tissue forms an oxygen-deficient environment due to its vigorous growth and metabolism. Many organic photosensitizers are difficult to produce singlet oxygen under hypoxic conditions, and can react with singlet oxygen, i.e., photobleaching, which reduces the photosensitizer activity. and ROS concentration, which significantly reduces the PDT efficacy [39-41]. Therefore, if the oxygen concentration can be increased during the PDT process, the PDT effect will be greatly improved. There is also a series of studies on solving the problem of lack of oxygen during PDT. And reports.

Achilefu's research group [42] connected ruthenium complex (N3) to titanium dioxide (TiO2) nanoparticles to form TiO2-N3 nanoparticles. Under light, N3 transferred electrons to TiO2, and at an oxygen concentration of 160 mmHg (1 mmHg = 133.2 Pa), it produced 3 and 4 times more hydroxyl radicals and hydrogen peroxide than TiO2 alone, respectively. Under anaerobic conditions , it could also produce 3 times more hydroxyl radicals than TiO2 alone, and the singlet oxygen yield remained basically unchanged. TiO2 nanoparticles connected with N3 converted the original singlet oxygen to The TiO2-based type II PDT is transformed into a type I PDT, which is less dependent on oxygen. Perfluorocarbons

(PFCs) have excellent oxygen carrying capacity. There are many studies that use perfluorocarbons to increase oxygen in the tumor site. The Hu research group [43] encapsulated the photosensitizer with perfluorocarbon nanoparticles and found that the photodynamic effect was greatly enhanced. Subsequently, the Hu research group[44] developed a new type of oxygen self-enriched bionic red blood cells (Biological red blood cells), can produce fluorescence, imaging-guided photothermal therapy and enhance the effect of photodynamic therapy. It consists of red blood cell membranes containing indocyanine green (ICG) and PFC and albumin nanoparticles (IPH). The red blood cell membrane is successfully coated After being attached to the nanoparticles, due to the retention of proteins in the red blood cell membrane, the biological red blood cells can effectively reduce the immune clearance rate of macrophages and prolong the circulation time in the body. The new type of biological red blood cells with longer lifespan and higher oxygen capacity can significantly In addition, high-capacity PFC can provide more oxygen, produce more 1 O2, prolong its life, and enhance the efficacy of PDT. Huang's research group [45] combined pentafluorophenyl and polyethylene glycol (PEG (PEG) was connected to porphyrin and found to improve hypoxia during PDT and enhance the PDT effect.

Zhang's group [46] synthesized a multifunctional nanocomposite (PCCN) based on carbon nanotubes (C3N4) with enhanced red absorption, which can be used for light-driven water decomposition to produce oxygen. Then, they synthesized C3N4 nanoparticles doped with polyethylene glycol segments containing protoporphyrin and targeted Arg-Gly-Asp motifs and introduced carbon dots. In vitro and in vivo experiments showed that they could increase the yield of reactive oxygen species and reverse PDT

tolerance caused by hypoxia. In order to minimize light-induced hypoxia, light can also be introduced intermittently (partial PDT) to allow cells to replenish oxygen. Therefore, Akkaya's group [47] used a 2-pyridone module to capture singlet oxygen. In the light cycle, the endoperoxide of 2-pyridone is produced together with singlet oxygen; in the dark cycle, the endoperoxide undergoes a thermal cycle to reverse the generation of singlet oxygen and the 2-pyridone module. **2.4.3** Illumination frequency The illumination

frequency affects the tissue penetration of light and the excitation of photosensitizers. Light with a wavelength biased towards the infrared, The stronger its tissue penetration, the less than 5 mm light penetration depth below 600 nm cannot be used for

deep tumors and have greater toxicity to tissues; and when the wavelength of light is 650~1000 nm . Shows good penetration . The wavelength range of 650-1000 nm is called the therapeutic window wavelength[48] . Photosensitizers within the therapeutic window have better PDT efficacy.

Upconversion nanoparticles (UCNPs) can absorb near-infrared light (NIR) The absorption is converted into UV-Vis emission and combined with the corresponding photosensitizer for PDT. The UCNP system[49] has a large conversion range and can convert from near infrared to shorter wavelengths of near infrared, near infrared to visible, and even near infrared to Ultraviolet emission, and the emitted light has the advantages of uninterrupted and non-scattering. Because NIR is a transparent window of biological tissue, NIR can penetrate deeper Penetrates tissues, while most photosensitizers have shorter excitation wavelengths (around 600 nm). Right), which requires UCNP to convert the wavelength of light. For example, TiO2 A large amount of ROS can be generated under the excitation of 275~390 nm light, which can encapsulate TiO2 UCNP can generate a large amount of ROS under longer wavelength excitation[50~52]. A UCNP doped with lanthanide element thulium (Tm) is used to encapsulate TiO2. UCNP can convert near-infrared light at a wavelength of 980 nm into ultraviolet light, which stimulates TiO2 to produce a large amount of ROS, especially O2 ·ÿ[27]. Loh's research group[53] Covalent binding of upconversion nanoparticles with the photosensitizer chlorin e6 (Ce6) can be used for deep tissue PDT. The drug loading capacity is very small, and the hydrophobic photosensitizer can rely on the intermolecular Adsorption connection. Liu's group[54] connected Ce6 with amphiphilic molecules The alkyl end of C18PMH-PEG was loaded to obtain UCNP-Ce6 molecules with It has a good PDT effect and can penetrate the 8 mm thick tissue and maintain 50% singlet oxygen yield. The research group [55] prepared UCNPs with positive charges on the surface of Ln3+, which can be used with Negatively charged carboxyl zinc phthalocyanine (ZnPc-COOH) adsorbs and binds 96.3% energy conversion efficiency. Modification of UCNP with polymer layer can To impart other functions, such as biocompatibility, in vivo stability or drug Delivery capability[56].

Two-photon absorption (TPA) refers to the superphoton absorption produced by pulsed lasers. At the focus of a strong laser, two photons can excite a molecule at the same time. The energy outside the point is not enough to produce two-photon absorption. The wavelength of light used for photon excitation is relatively long, with good tissue penetration and The corresponding single-photon process cannot occur, so the two-photon process has good Good spatial selectivity. The corresponding two-photon absorption photosensitizer also has There are more studies. There are photosensitizers that are directly excited by two-photons, and there are also The photosensitizer is indirectly activated by fluorescence resonance energy transfer (FRET) by exciting a substance with a large two-photon absorption cross section (TPACS).

Some rare metals (such as ruthenium, platinum, etc.) have two-photon absorption to produce Singlet oxygen properties, but these heavy metals are highly toxic and are not suitable for On the other hand, organic photosensitizers usually have lower two-photon absorption cross section (<50 GM), which requires the synthesis of some Conjugated photosensitizers can directly enhance the TPA cross section, or With a light-harvesting unit (e.g., polymer dots/semiconductor mass) having a large TPA The electron dots and gold nanostructures are combined.

The Chao group[57] synthesized a glutathione (GSH)-activated The photosensitization of ruthenium(II)-azo (Ru-azo) complex The agent can achieve two-photon excitation at 810 nm and single-photon excitation at 450 nm, and the double photons in the Ru-azo structure The nitrogen bond can only be reduced by glutathione. Strong fluorescence intensity and photodynamic effect, glutathione in tumor cells The peptide content is relatively high, which is more conducive to the incorporation of Ru-azo into tumor cells. In the absorption spectrum of Ru-azo, the maximum absorption wavelength is 572 and 450 nm, when GSH was added, the absorbance at 450 and 572 nm The concentration of GSH was gradually increased and decreased, respectively, and GSH was added at a molar ratio of 1:2. After that, the fluorescence emission intensity at 640 nm increased 50 times.

Qian's group[58] synthesized a red fluorescent Sensitizer tetraphenylethylene (TPE-red), compared with traditional Different from the aggregation quenching of , this photosensitizer has aggregation-induced emission[59] TPE-red is coated with polystyrene-maleic anhydride (PSMA) to form TPE-red-PSMA nanoparticles, which have a very high Large two-photon absorption cross section. Some photosensitizers have smaller TPACS, such as a porphyrin photosensitizer TPACS of 5,10,15,20-tetrakis (1-methyl 4-pyridinio) porphyrins (TMPyP)

The TPACS of carbon nanodots at 700 nm is 15000 GM, which is suitable for two-photon excitation.

Carbon quantum dots (CDot) and TMPyP are electrostatically bonded to form a CDot-TMPyP complex. Under the excitation of femtosecond laser, TMPyP is excited through FRET, and the singlet oxygen generated is more efficient than that of pure TMPyP.

Zhu's group [62] also used two-photon absorption hyperbranched covalent Hyperbranched conjugated polymer (HCP) core The HCP@HPE nanoparticles were successfully synthesized by combining the thermosensitive hyperbranched polyether (HPE) shell with the HCP@HPE nanoparticles. The NIR two-photon gating of the FRET process from HCP to Ce6 was demonstrated. **2.4.4** Photosensitizer singlet oxygen yield

The singlet oxygen yield of a photosensitizer is essentially determined by the photosensitizer structure. Studies have shown that the same photosensitizers with different modifications The singlet oxygen yield of the substituted radical will also change greatly. Introducing halogen atoms into the agent molecule can generally increase the ROS yield, such as Rhodamine and eosin, the structures of which are shown in Figure 4(a) and (b) Halogenation of the phthalocyanine ring can increase the ROS yield [18] . The introduction of Ag, Pd, Pt and other atoms into the center can also increase the ROS yield [18,63], such as diazaporphyrin and diazaporphyrin chelated with silver and copper atoms.

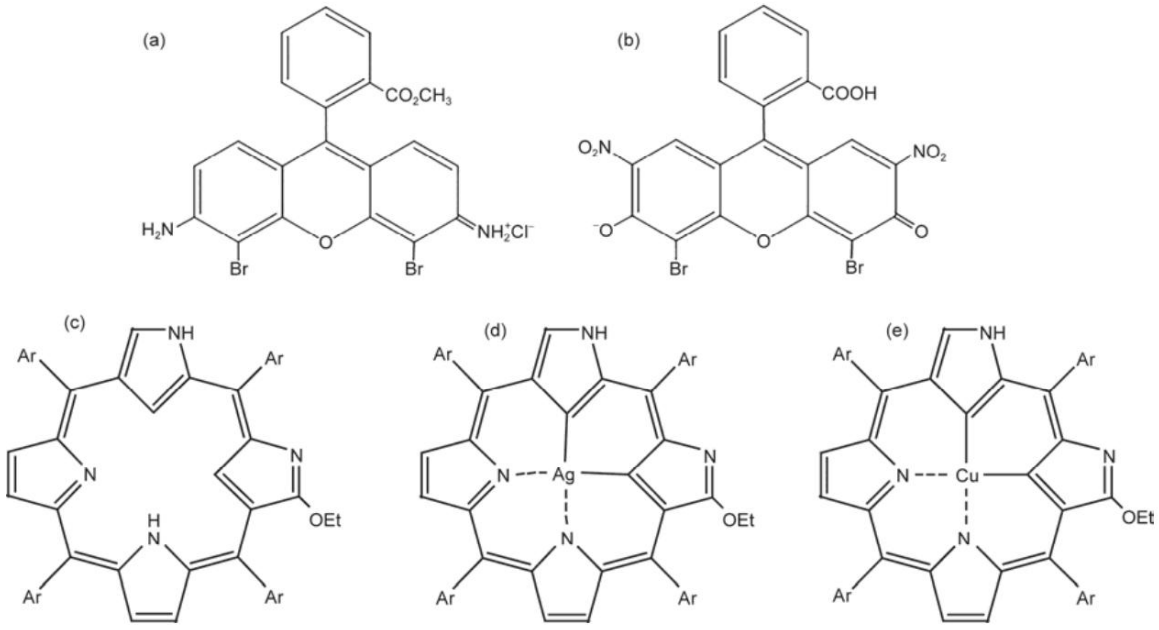

Figure **4** Photosensitizer structures. (a) Rhodamine; (b) Eosin; (c) Diazaporphyrin; (d), (e) Diazaporphyrin chelated with silver and copper atoms[18]

Figure 4 The structure of photosensitizer. (a) Dibromohodamine; (b) eosin; (c) doubly N-confused porphyrin; (d), (e) doubly N-confused porphyrin with metal complex[18]

The singlet oxygen yields are 0.19, 0.81, and 0.49, respectively. The structures are shown in the figure 4(c)~(e). Heavy

atoms can enhance spin-orbit coupling, thus facilitating intersystem hopping. This is called the "heavy atom effect".

In addition, iodine atoms show more effective heavy atom effects than other halogens. However, some studies have shown that excessive halogen atom-substituted boron-dipyrromethene (BODIPY) photosensitizes

However, increasing the halogen

The presence of fluorine atoms will also increase the dark toxicity of

photosensitizers[65]. Since most photosensitizers have a large conjugated structure, it is easy to

Aggregation, and the photosensitizer is exposed to an environment with high reactive oxygen concentration,

This will affect its stability, which will reduce the singlet oxygen yield of the photosensitizer.

However, a new type of photosensitizer can have aggregation

Based on the characteristics of aggregation induced emission (AIE), Liu's group[66]

synthesized such photosensitizer TPETCAQ, which has the following structure:

As shown in Figure 5, TPETCAQ has strong

The fluorescence of the fluorophore was not affected, and the singlet oxygen yield was not affected.

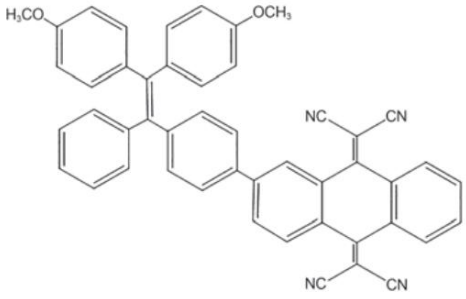

Figure **5** Structure of TPETCAQ[66]

Figure 5 The structure of TPETCAQ[66]

Compared with metal-free organic photosensitizers,

ROS[18] .Organometallic photosensitizers have longer triplet lifetimes and can

Increase its reaction with oxygen species and the generation of ROS[67], such as rose

Conditions for the presence of red (RB) in silver island films (SiFs)

The singlet oxygen yield was increased by 3 times compared with that of pure rose bengal.

A series of subsequent studies also obtained Ag, Au, Zn and Ni nanoparticles.

Increased singlet oxygen production[68,69]

The mixed metal photosensitizer composed of Au nanoparticles and ZnO

nanorods has the best singlet oxygen yield when the molar ratio of ZnO:Au is 20:1, at

which point ZnO and Au have the largest surface contact area[70].

Ru(II)(N3) has multiple triplet states, metal and ligand or ligand and ligand

There are many electron transfers between the two bodies. Currently, there are many ruthenium-containing

Photosensitizers are under research[71~75].

2.5 Other new photosensitizers and PDT technologies

2.5.1 Inorganic or organic metal photosensitizers

Metal nanoclusters, metal nanocrystals or metal nanoparticles can increase

Strong surface electromagnetic fields, surface plasmon resonance can increase the contact with the surface

Singlet oxygen yield of photosensitizers with metal centers

Graphene has strong absorption in the entire visible region to the near-infrared region. However, its high biological toxicity and low penetration of excitation light limit its clinical application. In an iron oxide-modified graphene oxide (GO-FexOH), electrons are transferred from GO to Fe(III) under the excitation of 808 nm light, accelerating the reaction with oxygen to form superoxide anions. Superoxide anions can also continue to undergo disproportionation reactions to form hydrogen peroxide. Hydrogen peroxide reacts with Fe(II) to produce hydroxyl radicals through the Fenton reaction, which can generate more ROS faster than pure GO[76]. **2.5.2** Combination of photodynamic therapy with chemotherapy or photothermal therapy

By using the principle that ROS can break specific covalent bonds or degrade polymers, chemotherapy drugs can be connected to photosensitizer nanoparticles through ROS-degradable materials, thus achieving ROS-induced controlled release of chemotherapy drugs and performing PDT and chemotherapy simultaneously. UCNP-wrapped SiO2 nanoparticles are connected to Rose Bengal (RB), and then doxorubicin (DOX) is loaded on biodegradable poly(1,4-phenyle-neacetone dimethylenethioketal) (PPADT) and self-assembled onto the nanoparticles. Under the excitation of NIR, the nanoparticles produce ROS, which can degrade PPADT and release DOX, achieving simultaneous chemotherapy and photodynamic therapy[77]. Photodynamic therapy can also be combined with photothermal therapy (PTT) to treat tumors to achieve the effect of combined promotion of treatment. The combination of the two can be referred to as combined phototherapy. Li's group[78] synthesized mesoporous SiO2 nanorods doped with gold nanorods and chlorin e6 (Ce6) (AuNRs-

Ce6-MSNRs), and achieved combined phototherapy under single-wavelength near-infrared light triggering, in which gold nanorods and Ce6 achieved the effects of PTT and PDT respectively. Liu's group[79] prepared polypyrrole (PPy) nanoparticles by using bovine serum albumin (BSA) pre-coupled with the photosensitizer chlorin e6 (Ce6) as a stabilizer. The obtained PPy@BSA-Ce6 nanoparticles can simultaneously trigger photodynamic therapy and photothermal therapy.

2.5.3 ROS controlled release photosensitizer

Some photosensitizers with ROS controlled release can specifically kill tumor cells while avoiding toxic side effects in other tissues. Polyethylene glycol-b-polycaprolactone bundles (PCL)[80] carry both the photosensitizer pheophorbide (PHA) and the singlet oxygen scavenger ÿ-carotene (CAR). When in non-tumor sites, CAR can scavenge the singlet oxygen produced by PHA, thereby reducing side effects. When in tumor sites, PCL biodegrades, PHA and CAR separate, and the singlet oxygen produced is not scavenged, killing tumor cells. **2.5.4** Fiber-optic delivery of photosensitizers

The Bartusik group[81] invented a lightweight optical fiber delivery device for photosensitizers. The optical fiber head is made of silicon fluoride mesoporous material. The photosensitive agent is connected to the optical fiber head through a bond that can be broken by light. Red light is delivered to the optical fiber head through the optical fiber to mediate the release of the photosensitizer. In addition, the optical fiber head also has the function of releasing oxygen to increase the local oxygen concentration. This technology has a killing range radius of 2~3 mm and is suitable for some small and difficult-to-remove tumors, such as brain tumors. **2.5.5** Fluorescent protein

Some modified fluorescent proteins

based on the basic chromophore structure of green fluorescent protein can not only emit fluorescence, but also generate ROS under light excitation. The most famous of these photodynamically active fluorescent proteins is called KillerRed. KillerRed is a unique red fluorescent protein that has the ability to generate ROS and excellent phototoxicity, and has the potential to be used as a photosensitizer in tumor treatment applications [82~84]. The expression location of the protein in the cell can be controlled by other genetic elements connected to the DNA sequence of the KillerRed molecule [21].

3. Detection of Reactive Oxygen Species

There are several methods for detecting and quantifying ROS in biological samples. One method for directly detecting singlet oxygen is phosphorescence spectrophotometry, which uses the phosphorescence emitted by singlet oxygen at 1270 nm [85]. There are also indirect detection methods based on probe molecules, mainly chemiluminescent probes and fluorescent probes. Although indirect detection signals are stronger and can be used for fluorescence microscopy, a major disadvantage of indirect methods is that they cannot resolve any dynamics that contain specific information about the surrounding environment. In heterogeneous systems in vivo, probe molecules and photosensitizers have different distribution forms and may react with proteins, etc., resulting in unreliable results. In addition, these probe molecules also have certain toxic side effects. Therefore, direct detection is particularly important, but direct detection also has a series of difficulties, such as low quantum yield and short singlet oxygen lifetime. Especially in the in vivo environment, the detection limit often does not meet the requirements, which is also a difficulty in the in vivo detection of reactive oxygen species. Although the in vivo detection of reactive oxygen species is difficult, real-time monitoring of blood oxygen levels during PDT has been achieved. It can also be used in preclinical or clinical research to guide the detection of blood oxygen levels to a certain extent.

PDT[86]. Since reactive oxygen species, especially singlet oxygen levels, only account for a small part of oxygen levels and can change greatly when conditions such as photosensitizers and light change, the reactive oxygen levels cannot be directly correlated with blood oxygen levels. It is therefore necessary to monitor reactive oxygen species in real time in vivo. The following will introduce methods for detecting singlet oxygen and other reactive oxygen species one by one.

3.1 Direct phosphorescence spectrophotometry

Direct phosphorescence is based on the emission of singlet oxygen when it returns to the ground state.

The singlet oxygen is detected by phosphorescence at 1270 nm. Due to the very low phosphorescence quantum yield, extremely high reactivity and extremely short lifetime of singlet oxygen, the phosphorescence signal at 1270 nm is extremely weak. Therefore, the phosphorescence signal must be amplified for direct detection. There are currently two methods for direct luminescence imaging of 1 O2: (1) Using NIR photomultiplier tubes (2) based on the use of a NIR camera with a filter [87].

Due to the short lifetime of singlet oxygen, time resolution is particularly important for direct phosphorescence, so time-resolved detection of O2 phosphorescence (TRPD) has emerged. There are basically three main photon counting techniques: gated photon counting (GPC), multi-channel counting (MCS) and time-correlated single photon counting (TCSPC) [88]. In TCSPC, only the first photon that hits

the detector in each laser irradiation can be counted. This method provides the most accurate photon timing of all photon counting techniques, down to a few picoseconds per channel. Therefore, when the time resolution requirement is very high, time-correlated single photon counting is the first choice, but only one photon is recorded for each laser pulse excitation, so a longer acquisition time is required to construct a complete signal profile. In GPC, a time window is first

set. Within the preset time window, all pulse signals exceeding the minimum threshold after the excitation pulse are counted. Repeated measurements at different time delays can establish the waveform. Gated photon counting is used to select only a portion of the total emitted photons. Typical applications are to distinguish between transient and delayed emission, for example to discriminate fluorescence from phosphorescence, or to remove scattered light after excitation. The main disadvantage of GPC is that it does not record the signal of all photons to be measured, but only counts the photons within the gate.

The MCS technique is similar to the GPC technique and can ultimately be viewed as a multi-gated photon counting technique that counts and sorts all detected photons at different locations in the on-board memory. The temporal distribution of all detected photons is thus obtained at once. The temporal resolution of the technique depends on the memory speed and is currently around 1 ns per channel, which is sufficient for singlet oxygen

detection [76]. Two different approaches can be used to condition the emission signal before it is sensed by the detector. One is to use a monochromator to resolve the sample's luminescence at the expense of signal intensity at the expense of sensitivity, and the other is to use bandpass filters and interference filters to provide the highest throughput at the expense of spectral resolution. Different approaches are suitable for different situations. In vivo time-resolved 1 O2 luminescence measurements remain very difficult and need to be improved to provide a diagnostic tool for clinical protocols or research [89]. InGaAs cameras have good photon detection efficiency (>30%) and large effective

On the other hand, PMTs are the detector of choice in many singlet oxygen experiments. Their main advantage is a large active area (>10 mm × 10 mm), which is necessary for collecting photons from large diffuse samples; however, they have very low quantum efficiency (<1%), moderate noise (>10,000 cps), a delicate photocathode (which can be damaged by ambient light), and difficulty in suppressing stray light by the detector during detection [90]. In different regions of the visible and low NIR spectrum (400–

1000 nm), silicon single-photon avalanche diodes (or semiconductor-based single-photon avalanche diodes, SPADS) are replacing PMTs because of their higher detection efficiency, lower noise, smaller size, and better gating. In the near-infrared wavelength range (1000–1700 nm), single-photon avalanche diode detectors are also an emerging technology, However, their use is hampered by high noise (dark count rate,

DCR) and the gating mode limitation with a maximum gate width of tens of nanoseconds [90].

The Hasan group[91] developed a new singlet oxygen detection (SOD) system based on photomultiplier tubes.
The lowest and highest 1 O2 concentrations detected by the PMT-SOD system were 15 nmol/L and 10 ÿmol/L, respectively. The Zbinden group[92] first proposed a time-resolved singlet oxygen luminescence detection device based on a semiconductor single-photon detector. Compared with superconducting detectors, it demonstrated a signal-to-noise ratio (SNR) improvement of more than 2 orders of magnitude. Compared with PMT, it has lower noise and higher quantum efficiency, allowing for shorter acquisition times and lower excitation powers

for in vivo measurements [92]. The negative-feedback InGaAs/InP avalanche diode (NFAD) detector[93] can achieve a DCR as low as 1 cps with an efficiency of 10%. Such a low DCR value can usually only be achieved by SNSPD. In addition, the detector proposed in this work is coupled to a large-area multimode optical fiber, which improves the in vivo and in vitro collection efficiency of biological samples. Compared with the previously reported single-mode fiber-coupled detector, the collection efficiency is 100 times higher than that of similar applications. The drive electronics are also designed to allow the detector to operate in either free-running mode (the detector is always on and ready to detect photons) or in gated mode (the detector can be selectively turned off to block unwanted light signals). The latter mode of operation is particularly useful when measuring sample singlet oxygen signals in the presence of a large number of stray photons from fluorescence.

The Hadfield group [23] is currently conducting similar research using gated Peltier-cooled InGaAs/InP single-photon avalanche diode detectors.

Such gated SPADs do not require the same cooling constraints as free-running SPADs, and use a compact Peltier cooling system rather than a bulky Stirling system, making them more portable, reliable, and practical. By synchronizing the detector with the frequency of the pump light source, a gating mode can be created so that the detector is active only during important time intervals (i.e., when 1 O2 produces a luminescence signal), thereby reducing the immediate luminescence background of the photosensitizer. The system is further enhanced by using a remote sensor head, in which the pump laser and luminescence signal are coupled into the optical fiber, allowing the detection and timing electronics to be located away from

the treatment site, as shown in Figure 6. The 523 nm laser is coupled into the delivery fiber through the collimating package (CP1) in the remote sensor head. The light from the collection fiber is coupled out through CP2 and passes through a bandpass filter (FW) and a longpass filter (LP, >1000 nm). The microscope objective (MO) images the fiber core onto the surface of the detector (Figure 6(a)). Figure 6(b) shows a schematic diagram of the sensor head with lenses (L1-L3) and a dichroic mirror (DM). The xy translation stage allows the two optical axes to be aligned on the sample. The electrical signal from the pulse pattern generator (PPG) (blue) triggers the release of two signals (red). One acts as the "start" signal for the TCSPC, and the other triggers the SPAD gating. The output from the SPAD (green) (which can only occur during the gating period) is sent to the TCSPC stop "channel" (Figure 6(c)). Detailed components and parameters are

described in reference [23]. The laser outputs a synchronized electrical signal to the programmable pulse pattern generator, and each pulse produces output on 2 independent channels, each channel

The first output is a single pulse sent to the synchronization or “start” channel of the time-correlated single-photon counter, while the second is a pulse pattern (with a frequency higher than the laser repetition rate) that is fed to the SPAD control module. Whenever the latter receives a pulse from the PPG, the SPAD is turned on for a predetermined duration, here called the gate width (usually much shorter than the laser period, about 24 ns). Any detection event (or dark count) that falls within this gate width outputs a pulse that stops the channel of the TCSPC. Any photons incident on the detector outside of the gate cannot be detected. This approach enables the generation of a timing histogram of detection events only within the preselected gate window; thus, photons detected in situations where there are only a few photons (e.g., near the end of the histogram) or where fluorescent photons would saturate the detector (at the beginning of the histogram) can be intentionally avoided. This strategy also reduces the overall count rate of the detector, helping to avoid pulse pile-up effects due to distorted histogram shapes, thereby reducing after-pulse effects that can increase background levels. This approach results in the inevitable loss of photon signal outside the detector gating cycle time; however, this signal loss appears to have no effect on data quality [23].

In addition to using photomultiplier technology to amplify phosphorescence signals, there are currently a series of other methods used to enhance 1270 nm phosphorescence emission. It has been reported that gold nanoparticles with appropriate surface plasmons can enhance the phosphorescence of 1 O2 by several hundred times [94]. Using the same plasmon principle, silver island films can also enhance the near-infrared phosphorescence of 1 O2 by 35 times [95].

Based on porous silicon microcavity (pSiMC)

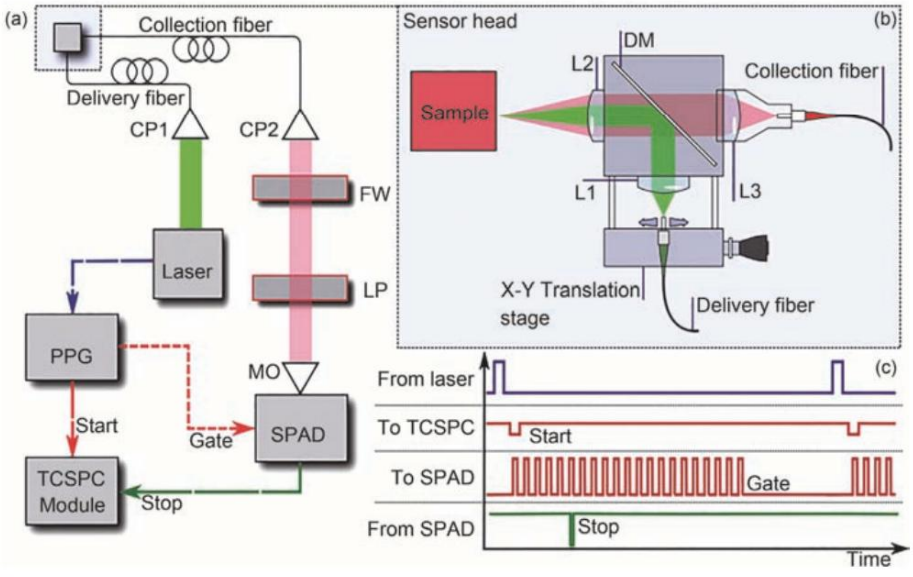

Figure **6** Block diagram of the experimental setup of SPAD. (a) Block diagram of the experimental setup; (b) Schematic diagram of the portable and compact sensor head; (c) Signal transmission pathway[23]

Figure 6 The block diagram of SPAD’s experimental device. (a) The block diagram of experimental device; (b) schematic of the portable compact sensor head; (c) signal transmission path[23]

The structure can enhance the luminescence of confined fluorescent groups. pSiMCs are a good host matrix for luminescent molecules because they can sharpen and amplify the emission. Voelcker's group [94] designed a europium (Eu)-based probe pSiMC-EuA for the detection of 1 O2. The probe EuA is composed of a highly emissive europium complex and a carborane dipole, which can overcome the inherent low molar absorptivity of europium and anthracene groups as chemical traps for 1 O2. Another method

for direct detection is delayed fluorescence detection. Singlet oxygen-sensitized delayed fluorescence (SOSDF) [96] is a delayed emission caused by the back transfer of energy from 1 O2 *to the S1 state of the photosensitizer.* Figure 7 describes the generation of delayed fluorescence. This is a common phenomenon for water-soluble photosensitizers. The SOSDF spectrum matches the immediate fluorescence spectrum, but occurs in the microsecond time range after the phosphorescence feature. SOSDF has characteristic rise-decay kinetics, and its analysis can provide information on the lifetime of 1 O2 and the triplet state of the photosensitizer. Since the photosensitizer itself acts as a specific 1 O2 probe, so SOSDF can be considered as a semi-direct method for 1 O2 detection, and SOSDF can provide similar kinetic parameters as direct 1 O2 detection. It is estimated that the emission intensity of SOSDF is several orders of magnitude higher than the 1 O2 phosphorescence intensity, but it is still several orders of magnitude weaker than the signal of indirect fluorescence probes [97,98].

3.2 Fluorescent probes and fluorescence spectrophotometry

Due to the quenching effect of photoinduced electron transfer, organic fluorescent probes themselves have no fluorescence. However, after reacting with singlet oxygen to form internal oxides, the probe molecules emit strong fluorescence[99]. Organic fluorescent probes are mainly fluorescein molecules bonded with anthracene derivatives. Currently, commercial fluorescent probes for singlet oxygen[100] include 9,10 -an-thracenedipropionic acid (APDA), singlet oxygen sensor green (SOSG), fluoresceinyl cypridina luciferin analogue (FCLA) and 1,3-diphenylisobenzofuran (DPBF). However, these probes are mainly used in homogeneous solution systems. Due to the complex environment in the body, the distribution and pharmacokinetic characteristics of the probes in the body, and their high potential toxicity, they are difficult to be used in the body.

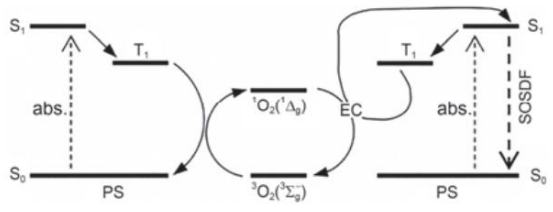

Figure **7** Principle of delayed fluorescence generation[96]

Figure 7 Delayed fluorescence generation principle[96]

Used for the quantification of singlet oxygen.

SOSG reacts with singlet oxygen to generate SOSG endoperoxide (SOSG-EP), which can be detected as fluorescent at 528 nm under 485 nm light excitation. However, SOSG can be activated by 530 nm light, acting as a photosensitizer to produce singlet oxygen and generate fluorescence, resulting in inaccurate results. Therefore, it is necessary to use this probe under appropriate conditions and with appropriate controls [101]. Nonell's group [102] developed a new singlet oxygen nanoprobe in which ADPA was covalently bound to mesoporous SiO2 nanoparticles to protect the probe from interaction with proteins.

The most popular chemical probe for measuring O2 ·ÿ in living cells is MitoSOX, which consists of a triphenylphosphonium ion (TPP+) covalently bound to a hydrocortisone molecule (HE). The probe fluoresces upon reaction with O2 ·ÿ .
TPP+ is a lipophilic cation that promotes mitochondrial uptake of HE based on the charge difference between the matrix and the intermembrane space. HE fluorescence is measured at an excitation wavelength of 396 nm [103].

The Birch-Machin group [104] developed an amperometric sensor functionalized with cytochrome c that can be used to measure the production of mitochondrial O2 in real time and can even detect O2 produced by mitochondrial complex II. O2 yellow fluorescent protein (cpYFP) can be stably expressed in cell systems or in vivo, and cpYFP can selectively target mitochondria through mitochondrial localization sequences. O2 ·ÿoxidizes the residues Cys171 and Cys193 in fluorescent proteins to cause fluorescence changes in cpYFP, which can be used to detect superoxide[105]. For

the detection of H2O2, Am-plex Red is the most commonly used method for accurately measuring H2O2 in isolated mitochondria . This method relies on the oxidation of non-fluorescent Amplex Red by H2O2 to produce fluorescent resorufin, which requires the presence of horseradish peroxidase [106]. Amplex Red analysis cannot be performed in intact tissue systems, but can be applied to tissues and cells. Another chemical method that can be used to detect mitochondrial H2O2 is the MitoB method[107]. This method relies on H2O2 to oxidize the aryl boronic acid MitoB to the corresponding fluorescently detectable phenol MitoP, in which the aryl boronic acid part is labeled with TPP+, which can achieve mitochondrial localization. Quantification of the MitoP/MitoB ratio by liquid chromatography-tandem mass spectrometry can measure the weighted average of mitochondrial H2O2 . Three highly sensitive fluorescent proteins have been developed. Allows

direct and indirect quantification of H2O2: HyPer, reduction-oxidation-sensitive green fluorescent protein-oxysterol-binding protein-related protein 1 (roGFP-Orp1) and recombinant human glutaredoxin-1-reduction-oxidation-sensitive green fluorescent protein

(Grx1-roGFP). HyPer was originally developed by Belousov et al. [108] and is composed of the prokaryotic H2O2 sensor protein OxyR and cyclic yellow fluorescent protein (cpYFP) conjugated. The change of HyPer fluorescence depends on Cys199 and Cys208 on OxyR. The oxidation of Cys199 in OxyR forms SOH,

Then SOH rapidly reacts with Cys208 to form an intramolecular disulfide bond, and H2O2 mediates the oxidation of OxyR, inducing changes in cpYFP fluorescence. Some studies have shown that HyPer is highly sensitive to changes in H2O2 due to the rapid reaction of Cys199 with H2O2. HyPer is now commonly used It is used to measure the dynamic changes of H2O2 in living cells, including cell signaling roGFP2-Orp1 directly detects H2O2, while Grx1-roGFP2 reacts with glutathione disulfide (GSSG) to induce apoptosis. It should be measured indirectly. GSSG is the product of two reduced glutathione molecules and The result of H2O2 enzyme-mediated oxidation. For roGFP2-Orp1, Orp1 The thiol anion is oxidized by H2O2 to form SOH, which then binds to the Orp1 The adjacent SH groups of roGFP2 react to form disulfide bridges. Through disulfide exchange reactions, the two thiols on roGFP2 are subsequently oxidized, thereby changing the fluorescence of the probe. Light intensity. Grx1-roGFP2 operates via a similar mechanism, except The increase in GSSG suggests that Grx1 undergoes an exchange reaction with thiol disulfide S-glutathione-Grx1-roGFP2 should be generated. The disulfide exchange reaction transfers the glutathione moiety to roGFP2, which then promotes the formation of disulfide bridges and changes the fluorescence of roGFP2. The needle has shown great potential in detecting the temporal and spatial changes of H2O2 in living animals. Great Hope[109].

H2-Calcein is different from dichlorodihydrofluorescein. H2-DCF is an excellent probe for intracellular ROS detection. The oxidized product calcein does not leak out of the cell and accumulates in the mitochondria, while dihydrofluorescein is located in the cytoplasm . It is the result of direct electron transfer to mitochondrial complex I [110]. Jelinek The research group[111] designed ascorbic acid derivatives embedded with amphiphilic carbon quantum dots. Biohydrogel, through the oxidation of ascorbic acid residues by ROS, leads to The disintegration of hydrogen-bonded hydrogel scaffolds and subsequent aggregation of carbon quantum dots led to fluorescence quenching for detecting reactive oxygen

species. Fluorescence based on a single wavelength may be affected by other biological matrices. In order to avoid this problem, many dual fluorescent probes are currently being used. It has been reported that dual fluorescent probes can emit fluorescence under the excitation of a single wavelength of light. The fluorescence of two wavelengths is emitted, and after reacting with active oxygen, one of them The fluorescence intensity of one wavelength changes, and the fluorescence intensity of another wavelength changes. By calculating the ratio of the two emission intensities, other factors can be avoided. The interference of SiO2 and gold nanoparticles on the signal makes the results more accurate. Nanocomposites composed of particles show single excitation and dual emission fluorescence Optical properties have been used to detect hydroxyl radicals[111].

The Kong group[5] first reported a method for detecting living cells Dual-emission ratiometric fluorescence of hydroxyl radicals in silicon quantum dots (Si QDs-Ce6) Nanocomposites, which combine silicon quantum dots (Si QDs) with Ce6-linked constructs can display well-resolved dual fluorescence emission signals (490 and 660 nm), the fluorescence of Si QDs can be quenched by OH, while Ce6 The fluorescence of Si QDs and Ce6 is measured at two wavelengths. The ratio of the intensities is used as a built-in correction to avoid environmental interference. A new fluorescent nanostructured ... Light ratiometric ROS detection system. After interacting with ROS, detection The red emission fluorescence (645 nm from QDs) in the system gradually decreased, while the green fluorescence (480 nm from AuNCs) did not change much. The fluorescence ratio of the long wavelength (I480 *nm/ I645* nm) is linearly correlated with the ROS content and can be used for real-time ratiometric detection of ROS. The results were similar to those of conventional dichlorofluorescein diacetate The results of the developed method are consistent with those of the salt method, which confirms the reliability of the developed method. The conjugates have high photostability, low background and ratiometric detection. The accuracy of the assay shows that it can be used as a real-time ROS detection probe in inflammatory cells. The potential of needles[112,113]. Peng's research group[6] synthesized a heterocyclic New cyanine staining with phenothiazine (PTZ-Cy2) The changes in absorption and fluorescence signals are This is due to the oxidation of the thiazine sulfur atom by hROS and the breaking of the cyanine ÿ bond conjugation. The double fluorescence emission at 470 and 595 nm is significantly enhanced. In aqueous solution, PTZ-Cy2 has a strong inhibitory effect on hROS compared with other ROS. Good fluorescence selectivity, and can also detect mitochondria in living cells Endogenous hROS production.

[1] Another major problem of O2 fluorescent probes is that they form complexes, affecting their response to 1 O2 and often preventing them Being taken up by cells. Making it into nanoparticles can effectively prevent the probe The molecules react with protein molecules and increase the cellular uptake rate, such as 9,10-anthraquinone acid (ADPA) covalently bound to porous silicon nanoparticle probes. needle, which has a high reactivity with singlet oxygen and can simultaneously Detection of singlet oxygen by changes in light and absorbance[102].

3.3 Chemical probe method

Chemical probes mainly refer to chemiluminescent probes. The probe reacts with singlet oxygen to produce a high-energy compound, which then rapidly Rapid decomposition releases energy in the form of light, or reacts with an initiator It emits a detectable light signal.

At present, the main chemiluminescent probes are those containing anthracene derivatives. Needle, such as 9-[2-(3-carboxy-9,10-dimethyl)anthracenyl]-6-hydroxy-3H-xanthanone Ton-3-one (DMAX), MTTA-Eu(III), MTDTA-Eu(III), etc. These chemical probes are initially non-luminescent. In the presence of 1 O2, These probes form endoperoxides at the 9,10 positions and emit light. In most cases, the quantum yield is 0.5~0.9[94,114]. The single oxygen chemiluminescence-cell penetrating peptide (SOCL-CPP)[115] can

Singlet oxygen reacts to produce phenolic dioxetane species, which then rapidly degrade in aqueous solution to produce the corresponding electronically excited benzoate, which emits 515 nm green light when decaying back to the ground state. Currently, the more successful active oxygen chemiluminescence assays include lucigenin, luminol, and jellyfish luciferin analog (CLA). Luminol, also known as luminol, can react with extremely small amounts of singlet oxygen to emit strong fluorescence. Lucigenin

chemiluminescence detection of O2 ·ÿ . It has good cell membrane permeability, low cytotoxicity, high reaction sensitivity and strong specificity. The reaction rate constant of O2·ÿ and lucigenin is three times that of O2 ·ÿ *and cytochrome c.* It can monitor O2·ÿ in real time in vascular endothelial cells, vascular smooth muscle cells, fibroblasts, renal cells, lymphocytes, alveolar epithelial cells, etc. [17]

There are also reports of probes that detect reactive oxygen species without chemiluminescence. These probes react with reactive oxygen species to change their structures, and quantify reactive oxygen species based on the ratio of their different structures. Lu's group [116] designed a peptide-based probe for rapid (<10 min) high-throughput measurement of reactive oxygen species induced by clinical drugs or in biological samples. They used matrix-assisted laser desorption ionization time-of-flight mass spectrometry (MALDI-TOF MS) to detect the ratio of different oxidation /reduction forms (including Cys-SOH/Cys-SH, CysSO2H/Cys-SH and Cys-SO3H/Cys-SH) of thiol (Cys-SH), subsulfonic acid (Cys-SOH), sulfinic acid (Cys-SO2H) and sulfonic acid (Cys-SO3H) in cysteine to assess the degree of oxidative stress in the sample.

3.4 Singlet oxygen detection based on molecular magnetism

The detection method based on molecular magnetic signals is electron spin resonance (ESR, EPR), which can detect compounds with unpaired electrons. A special singlet oxygen spin trap 2,2,6,6-tetramethyl-4-piperidine (TEMP) has been developed, which reacts with singlet oxygen to form a stable nitroxide radical 2,2,6,6-tetramethylpiperidine nitroxide (TEMPO), which can be measured using ESR. In the Bruker ELEXSYS E500 spectrometer, the theoretical detection limit of ESR is 4.0×10–12 mol . ESR is not only able to detect singlet oxygen, but also to quantify it with high sensitivity. However, the ESR signal is often affected by coexisting ions and solvents, which may lead to serious errors. When processing biological samples, several key factors need to be considered: (1) The presence of water causes the ESR signal to attenuate to a working limit of approximately 1×10ÿ9 mol. In order to further improve the EPR signal-to-noise ratio, Extraction methods must be developed to separate the ESR response from its aqueous environment; (2) many biomolecules can interact with the spin trap, so it is necessary to examine whether the trap has been modified; (3) the amount of spin trap penetration into the tissue is an important consideration, and it should be noted that not all spin traps function optimally at physiological pH [101]. Furthermore, the relative complexity of the analytical procedure

The high cost of the CoII complex and the expensive instruments also hinder its widespread application. The Que group [117] demonstrated the application of a single-nuclear high-spin CoII complex as a redox- active 19F MRI probe. The unpaired d electrons in the CoII center cause the paramagnetic relaxation enhancement (PRE) effect of the nearby 19F nucleus to attenuate the 19F NMR signal, resulting in a shortened T2 relaxation time. The CoII complex can be oxidized by H2O2 and other more active ROS to form a diamagnetic CoIII complex, and the T2 value will increase, generating a strong fluorine signal in NMR or 19F MRI, turning on the response to oxidation, and the oxidation is reversible, which can allow dynamic redox imaging. The Lutty group [118] developed a magnetic nanoparticle biosensor that can report the cellular response to oxidative stress through fluorescent proteins. This technology enables researchers to monitor ROS responses in real time using non-invasive microscopy.

3.5 Positron Emission Tomography

Positron emission tomography (PET) is a non-invasive imaging technique that can measure specific chemical or enzymatic reactions in tissues in vivo [119]. Due to its high sensitivity, low toxicity and high spatial resolution, PET has the potential to detect ROS[120]. Mach's group[119] synthesized a new 18F radiolabeled PET tracer, DHE analog, with a structure shown in Figure 8. It has good cell permeability when not oxidized, but can be selectively oxidized by superoxide anions to become positively charged, and has difficulty passing through cell membranes after oxidation. Wilson's group[120] used the reducing property of vitamin C to label it with 11C, which was oxidized to [11C]dehydroascorbic acid ([11C]DHA) under the action of ROS . There are also other reports using [11C] or [18F] labeled tracers for PET[121,122].

4 Mechanism of action of reactive oxygen species

Most studies believe that ROS destroy tumors mainly through the following three different mechanisms [123]: (1) direct toxicity to tumor cells, causing necrosis or inducing apoptosis and autophagy; (2) damage to tumor capillary endothelial cells and destruction of the microvasculature; (3) activation of acute inflammatory responses to host defense mechanisms. The following focuses on the effects of ROS on the immune system and tumor cell apoptosis pathways.

4.1 Effects on the immune system

Tissue damage to tumors caused by ROS leads to the release of damage-associated molecular patterns (DAMs).
DAMPs), such as calreticulin (CRT), high mobility group protein
(HMGB1), etc., like pathogen-associated molecular patterns (PAMPs) released by invasive pathogens

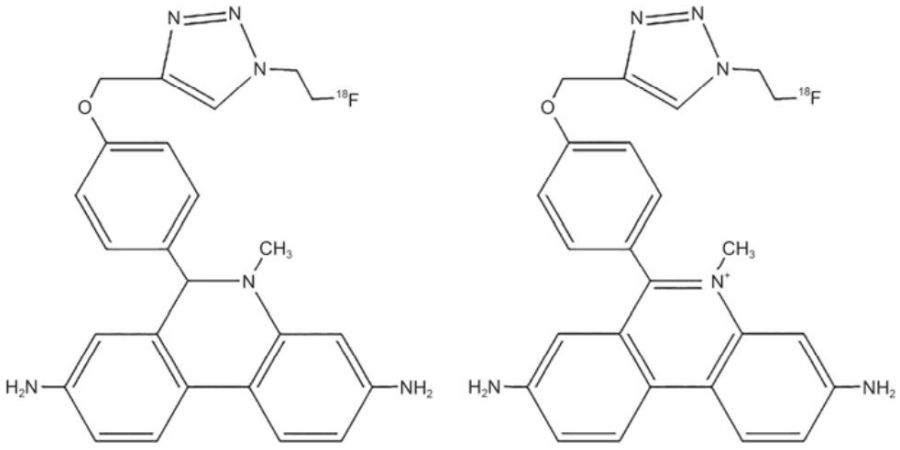

Figure **8** Structure of DHE analogs[119]

Figure 8 The structure of DHE analogue[119]

Activate host immune cells such as macrophages and neutrophils
Dendritic cells, etc., trigger adaptive immune responses.
DCs can take up antigens released by apoptotic tumor cells and migrate to
Draining lymph nodes, where they mature and transfer major histocompatibility
Major histocompatibility complex (MHC) molecules
The antigen-derived peptides are presented to T lymphocytes, which results in tumor-specific
CD4+ T helper cells (Th) and CD8+ cytotoxic T cells
Activation of cell toxic lymphoid T cells (CTL)[124]. After PDT
The most common DAMPs released are heat shock proteins HSP60, HSP70, HSP90 and
GRP94, which are upregulated and translocated to the cell membrane
[124,125]. In addition, ROS can induce MHC I expression on the surface of tumor cells.
ROS -induced ER stress can promote the intracellular trafficking of DAMPs/danger signals
and subsequent
Surface/extracellular expression[126].

ROS can also activate the complement system[123]. The complement cascade has three main
The main complement activation pathways are: classical pathway, alternative pathway and lectin pathway.
The alternative complement pathway is now considered to be the complement pathway associated with PDT.
PDT induces the cleavage of the unstable thioester bond in C3 through ROS to form a complementary
After binding to the cell membrane, C3b binds to the factor
In the presence of factor D, this complex will
is broken down into Ba and Bb. Bb will remain covalently bound to C3b to form
C3bBb, which is the alternative pathway C3 convertase. C3, C3b complex water
After decomposition, it becomes C3bBb3b, which splits C5 into C5a and C5b.
C6, C7, C8 and C9 complex (C5b6789) form the membrane attack complex
(MAC), which is inserted into the cell membrane, "punching holes" and triggering cell lysis.

4.2 Effects on cell apoptosis pathways

ROS can regulate a variety of apoptosis-related proteins in cells and activate apoptosis pathway, promoting apoptosis of tumor cells. Mitochondrial ROS burst can activate
Intrinsic membrane ion channel (IMAC), intracellular calcium concentration increases, line
Mitochondrial membrane potential decreases, *cytochrome c is released, and* caspases are activated
Caspase 3, 7, causes cell apoptosis, and activated caspase 3, 7 also
It can further promote the outbreak of ROS[27]. Chen's research group[28] found
After cytochrome c is released, B-cell lym-phoma-2 (Bcl-2) expression is downregulated
and Bax expression is upregulated, causing
Activation of caspase9, 12 and C/EBP homologous protein
The production of CHOP and glucose-regulated protein (GRP78) also increased.
Cytochrome c can also bind to apaf-1, and the binding complex recruits and activates
caspase 9. In the caspase-independent pathway
The mitochondria release apoptosis-inducing factor (AIF) and endonuclease G (Endo G),
which are then transported to the nucleus and induce chromatin condensation.

Inhibitors of apoptosis (IAPs) inhibit the endogenous expression of caspase 9
The increase of ROS activates p38 and
JNK MAPKs pathway, causing cell cycle arrest and ultimately inducing cell
Pretreatment with
a specific caspase-6 inhibitor abolished
PDT-induced lamin A/C cleavage and subsequent apoptosis, suggesting that ROS can
enhance the destruction of the nuclear lamins by activating caspase-6.

The Yin group[129]

Aloe-emodin (AE)-mediated photodynamic therapy
Effects of Aloe-emodin-mediated photodynamic therapy (AE-PDT) on human osteosarcoma
cell line MG-63 and its mechanism.
AE-PDT induced the expression of ROS and p-JNK.
N-acetyl-L-cysteine (NAC, 5 mmol/L) can block JNK-induced
Autophagy, apoptosis and phosphorylation of JNK, JNK inhibitor SP600125 (10

ÿmol/L) significantly inhibited the autophagy and apoptosis of MG63 cells induced by AE-PDT, proving the role of the ROS-JNK pathway in ROS-induced apoptosis. Lee's group [127] used low-energy proton beams to irradiate LLC, HepG2 and Molt-4 tumor cells and showed that the activity of caspase increased after irradiation. It also proved that p38 and JNK (not ERK) can be activated by ROS, thereby inducing apoptosis. Mitochondrial ROS (mitROS) is higher in tumor cells than in normal cells, inducing

Increase of Mn-SOD. Increased expression of heme transporter HCP1 in tumor cells. HCP1 is a transporter of porphyrin compounds. Its expression is higher in hypoxic tumors. Increased mitochondrial ROS induces the expression of pro-cancer factors, activation of transcription factor NF-kB, and expression of hypoxia-inducible factor 1ÿ (HIF-1ÿ), forming a tumor-specific phenotype, which is recognized and eliminated by the body's immune system [130]. In addition, HIF-1 transcriptional activity is strongly upregulated in PDT, inducing a PDT-resistant phenotype. RNAi knockdown of HIF-1 can reduce resistance to PDT. Activation of ERK1/2 mediated by oxidative stress after PDT involves positive regulation of HIF-1 transcriptional activity. Therefore, it is concluded that resistance to PDT is partly mediated by the activation of the ROS-ERK1/2-HIF-1 axis [131]. The sensitive to apoptosis gene (SAG, also known as RBX2 or ROC2) is a bifunctional protein. It has antioxidant activity when

present alone, and has E3 ligase activity when complexed with SCF-E3 (Skp1-cullins-F box proteins) ubiquitin ligase. Recent studies have shown that SAG siRNA silencing can increase the sensitivity of cancer cells to radiation, and the radiosensitization effect is related to the increase in the steady-state level of intracellular ROS. In addition, the elimination of Sag can reduce the degradation of nuclear factor inhibitor ÿ (IÿBÿ) and inhibit the activation of nuclear factor ÿB (NF-ÿB). IÿBÿ is a direct substrate of SAG-SCFÿ-TrCP E3 ubiquitin ligase. In summary, the increase in ROS levels and the inactivation of NF-ÿB increase the sensitivity of ES cells to radiation-induced cell death in which Sag has been eliminated [1322]. Zhou's research group [1333] reported that ROS generated by ALA-PDT stimulation caused the inhibition of the FGFR2b pathway downstream of PKC, resulting in a decrease in the expression of interleukin 1ÿ (IL-1ÿ), ultimately inhibiting the differentiation and proliferation of keratinocytes.

Yang's group[1344] studied the effect of upconversion fluorescent nanoparticles encapsulating chlorin e6 (UCNPs-Ce6)-mediated PDT on cholesterol efflux from THP-1 macrophage-derived foam cells and explored the potential of this approach. First, PDT was found to significantly enhance

Cholesterol efflux and autophagy induction in THP-1 and peritoneal macrophage-derived foam cells. The autophagy inhibitor 3-methyladenine and ATG5 siRNA significantly attenuated PDT-induced autophagy; subsequently,

ABCA1-mediated cholesterol efflux. In addition, reactive oxygen species (ROS) generated by PDT were responsible for the induction of autophagy, which could be blocked by the ROS inhibitor N-acetylcysteine (NAC). NAC could reverse PDT-induced p- Therefore, PDT promotes cholesterol efflux by inducing autophagy, which is partly mediated by the ROS/PI3K/Akt/mTOR signaling pathway in THP-1 and peritoneal macrophage-derived foam cells. Yang's group[49] also studied the effect of UCNPs-Ce6-mediated PDT on THP-1 macrophage apoptosis by promoting the production of reactive oxygen species (ROS). The results showed that the ROS level in the PDT group was significantly increased, leading to The mitochondrial sensitive transition pore (MPTP) opens, the mitochondrial membrane potential (MMP) depolarizes, and cytochrome c is released. The pro-apoptotic factor Bax then translocates from the cytoplasm to the mitochondria, cleaving caspase 9, cleaving caspase 3, and cleaving Therefore, UCNPs-Ce6 mediated PDT induced by ROS burst

Apoptosis of THP-1 macrophages.

5 Conclusion and Outlook

This article mainly discusses the research progress of reactive oxygen species in photodynamic therapy in recent years. In view of the poor targeting of photosensitizers in PDT, low local oxygen concentration in tumors, and weak light penetration, new photosensitizers and some newer PDT technologies that have emerged in recent years, such as upconversion systems, two-photon PDT, and fiber-delivered PDT, are introduced; in addition, new probes for singlet oxygen or other ROS detection and detectors that can be used to directly detect singlet oxygen phosphorescence, signal amplification and processing methods are also described; finally, the mechanism by which ROS promotes tumor cell apoptosis is explained, mainly including immune pathways and a series of apoptotic pathways in cells. Fluorescent molecular probes for highly sensitive detection of reactive oxygen species have been widely and deeply studied. Since each type of reactive oxygen species has its own unique physiological activity, the development of highly selective fluorescent probes that can detect a specific type of reactive oxygen species has become the current research frontier of biomedicine.

So far, there are only a few types of reactive oxygen species that can be directly measured, and the methods for direct measurement are also very limited. Due to the short lifespan and high reactivity of reactive oxygen species, the measurement of other reactive oxygen species, except H2O2, is still an international problem, and there is no particularly specific and effective method. However, in many fields such as biomedicine and environment, people are in urgent need of developing highly sensitive and highly selective reactive oxygen detection methods. In particular, the establishment of a simple and reliable in vivo detection method for reactive oxygen species is of great significance for biomedical research and the interpretation of various physiological and pathological phenomena of living organisms. With the development of technology, in the near future, it will be possible to achieve high-sensitivity and high-resolution in vivo real-time monitoring of ROS.

References

1 Liu Y Y, Wang X S, Zhang B W. Hypocrellin-based photodynamic sensitizers (in Chinese). Prog Chem, 2008, 20: 1345–1352 [ÿÿÿ, Wang Xuesong, Zhang Baowen. Hypocrellin-based photodynamic drugs. Progress in Chemistry, 2008, 20: 1345–1352]

2 Ogilby P R. Singlet oxygen: There is indeed something new under the sun. Chem Soc Rev, 2010, 41: 3181–3209 3 Ethirajan M, Chen Y, Joshi P, et al. ChemInform abstract: The role of porphyrin chemistry in tumor imaging and photodynamic therapy. Chem Soc Rev, 2011, 42: 340–362

4 Yang J. Chemical modification of bacterial chlorophyll and its PDT performance (in Chinese). Master Dissertation. Taiyuan: Shanxi Yang Jin. Chemical modification of bacterial chlorophyll and its PDT performance. Master's degree thesis. Taiyuan: Shanxi University, 2008

5 Zhao Q, Zhang R, Ye D, et al. A ratiometric fluorescent silicon quantum dots-Ce6 complex probe for the live cell imaging of highly reactive oxygen species. ACS Appl Mater Interfaces, 2017, 9: 2052–2058

6 Liu F, Wu T, Cao J, et al. A novel fluorescent sensor for detection of highly reactive oxygen species, and for imaging such endogenous hROS in the mitochondria of living cells. Analyst, 2013, 138: 775–778

7 Wang D, Zhao L, Guo L H, et al. Online detection of reactive oxygen species in ultraviolet (UV)-irradiated nano-TiO2 suspensions by continuous flow chemiluminescence. Anal Chem, 2014, 86: 10535–10539

8 La Favor J D, Anderson E J, Hickner R C. Novel method for detection of reactive oxygen species *in vivo* in human skeletal muscle. Physiol Res, 2014, 63: 387–392 9

Vatansever F, De Melo W C M A, Avci P, et al. Antimicrobial strategies centered around reactive oxygen species-bactericidal antibiotics, photodynamic therapy, and beyond. FEMS Microbiol Rev, 2013, 37: 955–989

10 Sarniak A, Lipiÿska J, Tytman K, et al. Endogenous mechanisms of reactive oxygen species (ROS) generation. Postepy Hig Med Dosw, 2016, 70: 1150–1165

11 Li W, Tan G, Zhang H, et al. Folate chitosan conjugated doxorubicin and pyropheophorbide acid nanoparticles (FCDP-NPs) for enhance photodynamic therapy. RSC Adv, 2017, 7: 44426–44437 12

Grivennikova V G, Vinogradov A D. Mitochondrial production of reactive oxygen species. Am J Physiol, 2013, 78: 1490–1511 13 Jayapaul J, Arns S, Lederle W, et al. Riboflavin carrier protein-targeted fluorescent USPIO for the assessment of vascular metabolism in tumors. Biomaterials, 2012, 33: 8822–8829

14 Yang M Y, Chang C J, Chen L Y. Blue light induced reactive oxygen species from flavin mononucleotide and flavin adenine dinucleotide on lethality of HeLa cells. J Photochem Photobiol B, 2017, 173: 325–332

15 Ekoue D N, He C, Diamond A M, et al. Manganese superoxide dismutase and glutathione peroxidase-1 contribute to the rise and fall of mitochondrial reactive oxygen species which drive oncogenesis. Biochem Biophys Acta Bioenerget, 2017, 1858: 628–632 16 Kirkinezos I G, Moraes C T. Reactive oxygen species and mitochondrial diseases. Semin Cell Dev Biol, 2001, 12: 449–457 17 Fan L M, Li J M. Evaluation of methods of detecting cell reactive oxygen species production for drug screening and cell cycle studies. J Pharmacol Toxicol, 2014, 70: 40–47

18 Mehraban N, Freeman H S. Developments in PDT sensitizers for increased selectivity and singlet oxygen production. Materials, 2015, 8: 4421–4456

19 Gao Y, Qia G M, Li N, et al. Progress of photosensitizer for cancer diagnosis and therapy. Chin J Anal Chem, 2011, 39: 1926–1931

20 Güzel E, Günsel A, Bilgiçli A T, et al. Synthesis and photophysicochemical properties of novel thiadiazole-substituted zinc(II), gallium(III) and silicon(IV) phthalocyanines for photodynamic therapy. Inorg Chem Acta, 2017, 467: 169–176

21 Kou J, Dou D, Yang L. Porphyrin photosensitizers in photodynamic therapy and its applications. Oncotarget, 2017, 8: 81591–81603

22 Abrahamse H, Hamblin M R. New photosensitizers for photodynamic therapy. Biocheml J, 2016, 473: 347–364 23 Gemmell N R, Mccarthy A, Kim M M, et al. A compact fiber-optic probe-based singlet oxygen luminescence detection system. J Biophoton, 2017, 10: 320–326

24 Rubio N, Fleury S P, Redmond R W. Spatial and temporal dynamics of *in vitro* photodynamic cell killing: Extracellular hydrogen peroxide mediates neighbouring cell death. Photochem Photobiol Sci, 2009, 8: 457–464

25 Zhao H, Xing D, Chen Q. New insights of mitochondria reactive oxygen species generation and cell apoptosis induced by low dose photodynamic therapy. Eur J Cancer, 2011, 47: 2750–2761

26 Hu Z, Ying S, Kon O L, et al. Unique triphenylphosphonium derivatives for enhanced mitochondrial uptake and photodynamic therapy. Bioconjugate Chem, 2017, 28: 590–599

27 Yu Z, Sun Q, Pan W, et al. A near-infrared triggered nanophotosensitizer inducing domino effect on mitochondrial reactive oxygen species burst for cancer therapy. ACS Nano, 2015, 9: 11064–11074

28 Li D, Li L, Li P, et al. Apoptosis of HeLa cells induced by a new targeting photosensitizer-based PDT via a mitochondrial pathway and

ER stress. Oncotargets Ther, 2015, 8: 703–711
29 Moromizato S, Hisamatsu Y, Suzuki T, et al. Design and synthesis of a luminescent cyclometalated Iridium(III) complex having N, N-diethylamino group that stains acidic intracellular organelles and induces cell death by photoirradiation. Inorg Chem, 2012, 51: 12697–12706 30 Nakagawa A, Hisamatsu Y, Moromizato S, et al. Synthesis and photochemical properties of pH responsive tris-cyclometalated iridium(III) complexes that contain a pyridine ring on the 2-phenylpyridine ligand. Inorg Chem, 2014, 53: 409–422
31 Koo H, Lee H, Lee S, et al. *In vivo* tumor diagnosis and photodynamic therapy via tumoral pH-responsive polymeric micelles. Chem Commun, 2010, 46: 5668–5670
32 Mitsunaga M, Ogawa M, Kosaka N, et al. Cancer cell-selective *in vivo* near infrared photoimmunotherapy targeting specific membrane molecules. Nat Med, 2011, 17: 1685–1691
33 Bryden F, Maruani A, Rodrigues J M M, et al. Assembly of high-potency photosensitizer-antibody conjugates through application of dendron multiplier technology. Bioconjugate Chem, 2017, 29: 176–181
34 Debele T A, Mekuria S L, Tsai H C. A pH-sensitive micelle composed of heparin, phospholipids, and histidine as the carrier of photosensitizers: Application to enhance photodynamic therapy of cancer. Int J Biol Macromol, 2017, 98: 125–138
35 Varchi G, Rapozzi V, Ragno D, et al. Androgen receptor targeted conjugate for bimodal photodynamic therapy of prostate cancer *in vitro.* Bioconjugate Chem, 2015, 26: 1662–1671
36 Le F G, Sol V, Ouk C, et al. Enhanced photobactericidal and targeting properties of a cationic porphyrin following attachment of Polymyxin B. Bioconjugate Chem, 2017, 28: 2493–2506
37 Chitgupi U, Zhang Y, Chi Y L, et al. Sulfonated-polyethyleneimine for photosensitizer conjugation and targeting. Bioconjugate Chem, 2015, 26: 1633–1639
38 Wen A M, Lee K L, Cao P, et al. Utilizing viral nanoparticle/dendron hybrid conjugates in photodynamic therapy for dual delivery to macrophages and cancer cells. Bioconjugate Chem, 2016, 27: 1227–1235
39 Mitra S, Foster T H. *In vivo* confocal fluorescence imaging of the intratumor distribution of the photosensitizer mono-L-aspartylchlorin-e6. Neoplasia, 2008, 10: 429–438
40 Celli J P, Spring B Q, Rizvi I, et al. Imaging and photodynamic therapy: Mechanisms, monitoring, and optimization. Chem Rev, 2010, 110: 2795–2838
41 Obaid G, Broekgaarden M, Bulin A L, et al. Photonanomedicine: A convergence of photodynamic therapy and nanotechnology. Nanoscale, 2016, 8: 12471–12503
42 Gilson R, Black K, Lane D D, et al. Hybrid TiO2-ruthenium nano-photosensitizer synergistically produces reactive oxygen species in both hypoxic and normoxic conditions. Angew Chem, 2017, 56: 10717–10720
43 Cheng Y, Hao C, Jiang C, et al. Perfluorocarbon nanoparticles enhance reactive oxygen levels and tumour growth inhibition in photodynamic therapy. Nat Commun, 2015, 6: 8785–8792
44 Ren H, Liu J, Li Y, et al. Oxygen self-enriched nanoparticles functionalized with erythrocyte membranes for long circulation and enhanced phototherapy. Acta Biomater, 2017, 59: 269–282
45 Que Y, Liu Y, Tan W, et al. Enhancing photodynamic therapy efficacy by using fluorinated nanoplatform. ACS Macro Lett, 2016, 5: 168–173 46 Zheng D W, Li B, Li C X, et al. Carbon-dot-decorated carbon nitride nanoparticles for enhanced photodynamic therapy against hypoxic tumor via water splitting. ACS Nano, 2016, 10: 8715–8722 47
Turan I S, Yildiz D, Turksoy A, et al. A bifunctional photosensitizer for enhanced fractional photodynamic therapy: Singlet oxygen generation in the presence and absence of light. Angew Chem, 2016, 128: 2925–2928
48 Nyokong T, Ahsen V. Photosensitizers. In: Medicine, Environment, and Security. Netherlands: Springer, 2012. 4: 315–349 49 Zhu X, Wang H, Zheng L, et al. Upconversion nanoparticle-mediated photodynamic therapy induces THP-1 macrophage apoptosis via ROS bursts and activation of the mitochondrial caspase pathway. Int J Nanomed, 2015, 10: 3719–3736
50 Zhou Z, Song J, Nie L, et al. Reactive oxygen species generating systems meeting challenges of photodynamic cancer therapy. Chem Society Rev, 2016, 45: 6597–6626
51 Idris NM, Sasidharan LS, Li Z, et al. Photoactivation of core-shell titania coated upconversion nanoparticles and its effect on cell death. J Mater Chem B, 2014, 2: 7017–7026
52 Lucky S S, Muhammad I N, Li Z, et al. Titania coated upconversion nanoparticles for near-infrared light triggered photodynamic therapy. ACS Nano, 2015, 9: 191–205
53 Dou Q Q, Teng C P, Ye E, et al. Effective near-infrared photodynamic therapy assisted by upconversion nanoparticles conjugated with photosensitizers. Int J Nanomed, 2015, 10: 419–432
54 Wang C, Tao H, Cheng L, et al. Near-infrared light induced in vivo photodynamic therapy of cancer based on upconversion nanoparti-cles. Biomaterials, 2011, 32: 6145–6154 55 Wang M, Chen Z, Zheng W, et al. Lanthanide-doped upconversion nanoparticles electrostatically coupled with photosensitizers for near-infrared-triggered photodynamic therapy. Nanoscale, 2014, 6: 8274–8282

56 Bagheri A, Arandiyan H, Adnan N N M, et al. Controlled direct growth of polymer shell on upconversion nanoparticle surface via visible light regulated polymerization. Macromolecules, 2017, 50: S1–S14
57 Zeng L, Kuang S, Li G, et al. A GSH-activatable ruthenium(II)-azo photosensitizer for two-photon photodynamic therapy. Chem Comwill, 2017, 53: 1977–1980
58 Alifu N, Dong X, Li D, et al. Aggregation-induced emission nanoparticles as photosensitizer for two-photon photodynamic therapy. Ma-ter Chem Frontiers, 2017, 1: 1746–1753 59 Li M. Design of nano-
fluorescent probes based on AIE luminescence mechanism and study on targeted imaging of tumor cells (in China). Doctoral Dissertation. Wuhan: Huazhong University of Science and Technology, 2013.
Design of optical probes and research on targeted imaging of tumor cells. PhD dissertation. Huazhong University of Science and Technology, 2013]
60 Cui C L. Synthesis and properties of novel fluorescent chemical sensors (in Chinese). Master Dessertation. Qingdao: Qingdao University of Science and Technology, 2010
61 Wang J, Zhang Z, Zha S, et al. Carbon nanodots featuring efficient FRET for two-photon photodynamic cancer therapy with a low fs laser power density. Biomaterials, 2014, 35: 9372–9381
62 Yu H, Feng Q, Shen L, et al. Combining two-photon activated fluorescence resonance energy transfer and near infrared photothermal effect of unimolecular micelles for enhanced photodynamic therapy. ACS Nano, 2016, 10: 10489–10499
63 Patel N J, Chen Y, Joshi P, et al. Effect of metalation on porphyrin-based bifunctional agents in tumor imaging and photodynamic therapy. Bioconjugate Chem, 2016, 27: 667–680
64 Zou J, Yin Z, Ding K, et al. BODIPY derivatives for photodynamic therapy: Influence of configuration versus heavy atom effect. ACS Appl Mater Interfaces, 2017, 9: 32475–32481
65 Watley R L, Awuah S G, Bio M, et al. Dual functioning thieno-pyrrole fused BODIPY dyes for NIR optical imaging and photodynamic therapy: singlet oxygen generation without heavy halogen atom assistance. Chem Asian J, 2015, 10: 1335–1343
66 Wu W, Mao D, Hu F, et al. A highly efficient and photostable photosensitizer with near-infrared aggregation-induced emission for image-guided photodynamic anticancer therapy. Adv Mater, 2017, 29: 1700548
67 Lincoln R, Kohler L, Monro S, et al. Exploitation of long-lived 3IL excited states for metal-organic photodynamic therapy: Verification in a metastatic melanoma model. J Am Chem Soc, 2013, 135: 17161–17175
68 Zhang Y, Aslan K, Previte M J, et al. Metal-enhanced singlet oxygen generation: A consequence of plasmon enhanced triplet yields. J Fluoresc, 2007, 17: 345–349
69 Pfau R, Tzatsos A, Kampranis S C, et al. Members of a family of JmjC domain-containing oncoproteins immortalize embryonic fibroblasts via a JmjC domain-dependent process. Proc Natl Acad Sci USA, 2008, 105: 1907–1912
70 Kang Z, Yan X, Zhao L, et al. Gold nanoparticle/ZnO nanorod hybrids for enhanced reactive oxygen species generation and photodynamic therapy, Nano Res, 2015, 8: 2004–2014
71 Fantacci S, De A F, Selloni A. Absorption spectrum and solvatochromism of the [Ru(4,4'-COOH-2,2'-bpy)2(NCS)2] molecular dye by time dependent density functional theory. J Am Chem Soc, 2003, 125: 4381–4387
72 Teles J, Pina J, Ribeiro C, et al. PEG-containing Ruthenium phthalocyanines as photosensitizers for photodynamic therapy: Synthesis, characterization and *in vitro* evaluation. J Mater Chem B, 2017, 5: 5862–5869
73 Hess J, Huang H, Kaiser A, et al. Evaluation of the medicinal potential of two Ruthenium(II) polypyridine complexes as one- and two-photon photodynamic therapy photosensitizers. Chemistry, 2017, 23: 9888–9896
74 Rui C, Zhang J, Chelora J, et al. Ruthenium(II) complex incorporated UiO-67 metal-organic frameworks nanoparticles for enhanced two-photon fluorescence imaging and photodynamic cancer therapy. ACS Appl Mater Interfaces, 2017, 9: 5699–5708 75 Gupta J,
Mohapatra J, Bahadur D. Visible light driven mesoporous Ag-embedded ZnO nanocomposites: Reactive oxygen species enhanced photocatalysis, bacterial inhibition and photodynamic therapy. Dalton Trans, 2017, 46: 685–696
76 He Y, Del V A, Qian Y, et al. Near infrared light-mediated enhancement of reactive oxygen species generation through electron transfer from graphene oxide to iron hydroxide/oxide. Nanoscale, 2016, 9: 1559–1566
77 Zhou F, Zheng B, Zhang Y, et al. Construction of near-infrared light-triggered reactive oxygen species-sensitive (UCN/SiO2-RB+DOX)@PPADT nanoparticles for simultaneous chemotherapy and photodynamic therapy. Nanotechnology, 2016, 27: 235601 78 Li L, Cho
H, Yoon K H, et al. Antioxidant-photosensitizer dual-loaded polymeric micelles with controllable production of reactive oxygen species. Int J Pharm, 2014, 471: 339–348
79 Sun Q, You Q, Pang X, et al. A photoresponsive and rod-shape nanocarrier: Single wavelength of light triggered photothermal and pho-todynamic therapy based on AuNRs-capped & Ce6-doped mesoporous silica nanorods. Biomaterials, 2017, 122: 188–200 80 Bartusik D, Aebisher D,
Ghogare A, et al. A fiberoptic (photodynamic therapy type) device with a photosensitizer and singlet oxygen delivery probe tip for ovarian cancer cell killing. Photochem Photobiol, 2013, 89: 936–941
81 Song X, Liang C, Gong H, et al. Photosensitizer-conjugated albumin-polypyrrole nanoparticles for imaging-guided *in vivo* photodynamic/photothermal therapy. Small, 2015, 11: 3932–3941

82 Sha S, Qin L, Wang A, et al. Metabolic imaging of the tumor treated by KillerRed fluorescent protein-based photodynamic therapy in mice. Int Soc Optics Photon, 2014: 89440T
83 Takehara K, Tazawa H, Hashimoto Y, et al. Abstract 706: A novel photodynamic therapy with virus-mediated delivery of photosensitive cytotoxic fluorescent protein KillerRed for human cancers. Cancer Res, 2014, 74: 706
84 Liao Z X, Kempson I M, Fa Y C, et al. Magnetically guided viral transduction of gene-based sensitization for localized photodynamic therapy to overcome multidrug resistance in breast cancer cells. Bioconjugate Chem, 2017, 28: 1702–1708
85 Schlothauer J, Röder B, Hackbarth S, et al. *In vivo* detection of time-resolved singlet oxygen luminescence during PDT is relevant conditions. Int Soc Optic Eng, 2010, 7551: 484–490
86 Wang M X, Dai Z F. Advances in equipment for tumor photodynamic therapy (in Chinese). Chin Sci Bull, 2017, 62: 1591–1601 [ÿÿÿ, Dai Z. F. Research progress of cancer photodynamic therapy. Chinese Science Bulletin, 2017, 62: 1591–1601]
87 Lin L, Chen L, Wang M, et al. Direct imaging of singlet oxygen luminescence generated in blood vessels during photodynamic therapy. In: Popp J, Tuchin V V, Matthews D L, eds. Biophotonics: Photonic Solutions for Better Health Care IV. Bellingham: SPIE-The Interna-tional Society for Optical Engineering, 2014. 9129: 912920 88 Jimã©Nez-Banzo
A, Ragã s X, Kapusta P, et al. Time-resolved methods in biophysics. 7. Photon counting vs. analog time-resolved singlet oxygen phosphorescence detection. Photochem Photobiol, 2008, 7: 1003–1010
89 Schlothauer JC, Hackbarth S, Jäger L, et al. Time-resolved singlet oxygen luminescence detection during photodynamic therapy is relevant conditions: comparison of *ex vivo* application of two photosensitizer formulations. J Biomed Opt, 2012, 17: 115005
90 Boso G, Ke D, Korzh B, et al. Time-resolved singlet-oxygen luminescence detection with an efficient and practical semiconductor single-photon detector. Biomed Optic Express, 2015, 7: 211–224 91
Kim I W, Park J M, Roh Y J, et al. Direct measurement of singlet oxygen by using a photomultiplier tube-based detection system. J Photochem Photobiol B, 2016, 159: 14–23
92 Boso G, Korzh B, Zbinden H. Low noise InGaAs/InP single-photon negative feedback avalanche diodes: Characterization and applications. In: Itzler M A, Campbell J, eds. Advanced Photon Counting Techniques IX. Bellingham: SPIE-International Society of Optical Engineering, 2015. 9492: 94920Q
93 Boso G, Korzh B, Sanguinetti B, et al. Low noise InGaAs/InP single-photon detector for singlet oxygen detection. In: Razeghi M, Tour-nie E, Brown G J, eds. Quantum Sensing and Nanophotonic Devices XII. Bellingham: SPIE-International Society of Optical Engineering, 2015. 9370: 93701S
94 Sna J, Plush S E, Voelcker N H. Singlet oxygen detection on a nanostructured porous silicon thin film via photonic luminescence enhancements. Langmuir, 2017, 33: 8606–8613
95 Ragàs X, Gallardo A, Zhang Y, et al. Singlet oxygen phosphorescence enhancement by silver islands films. J Phys Chem C, 2011, 115: 16275–16281
96 Scholz M, Biehl A L. The singlet-oxygen-sensitized delayed fluorescence in mammalian cells: A time-resolved microscopy approach. Photochem Photobiol Sci, 2015, 14: 700–713
97 Maryakhina V S, Letuta S N. Pathology development stage and its influence on the delayed fluorescence kinetics of molecular probes. Laser Phys, 2013, 23: 54–58
98 Letuta SN, Kuvandykova AF, Pashkevich SN, et al. Features of the delayed fluorescence kinetics of exogenous fluorophores in biological tissues. Russ J Phys Chem A, 2013, 87: 1582–1587 99 Yin Y J. Synthesis and
application of singlet oxygen-specific ruthenium complex phosphorescence probes (in Chinese). Master Dessertation. Dalian: Dalian University of Technology, 2012
Dissertation. Dalian: Dalian University of Technology, 2012]
100 Li B H, Lin H Y, Chen D F, et al. Singlet oxygen detection during photosensitization. J Innov Optic Health Sci, 2013, 6: 1330002 101 Koh E, Fluhr
R. Singlet oxygen detection in biological systems: Uses and limitations. Plant Signal Behav, 2016, 11: e1192742 102 Bresolí-Obach R, Nos J,
Mora M, et al. Anthracene-based fluorescent nanoprobes for singlet oxygen detection in biological media. Methods, 2016, 109: 64–72
103 Kalyanaraman B. Oxidative chemistry of fluorescent dyes: Implications in the detection of reactive oxygen and nitrogen species. Biochem Soc Transact, 2011, 39: 1221–1225
104 Henderson J R, Swalwell H, Boulton S, et al. Direct, real-time monitoring of superoxide generation in isolated mitochondria. Free Radic Res, 2009, 43: 796–802
105 Schwarzländer M, Logan D C, Fricker M D, et al. The circularly permuted yellow fluorescent protein cpYFP that has been used as a su-peroxide probe is highly responsive to pH but not superoxide in mitochondria: Implications for the existence of superoxide “flashes”. Biochem J, 2011, 437: 381–387
106 Starkov A A. Measurement of mitochondrial ROS production. Methods Mol Biol, 2010, 648: 245–255

107 Cochemé H M, Quin C, Mcquaker S J, et al. Measurement of H2O2 within living Drosophila during aging using a ratiometric mass spectrometry probe targeted to the mitochondrial matrix. Cell Metab, 2011, 13: 340–350
108 Belousov V, Fradkov A, Lukyanov K, et al. Genetically encoded fluorescent indicator for intracellular hydrogen peroxide. Nat Methods, 2006, 3: 281–286
109 Mailloux R J. Teaching the fundamentals of electron transfer reactions in mitochondria and the production and detection of reactive oxygen species. Redox Biol, 2015, 4: 381–398
110 Keller A, Mohamed A, Dröse S, et al. Analysis of dichlorodihydrofluorescein and dihydrocalcein as probes for the detection of intracellular reactive oxygen species. Free Radical Res, 2004, 38: 1257–1267
111 Bhattacharya S, Sarkar R, Nandi S, et al. Detection of reactive oxygen species by a carbon-dot-ascorbic acid hydrogel. Anal Chem, 2016, 89: 830–836
112 Ma Y, Wang Q, Zhu Q, et al. Dual fluorescence nano-conjugates for ratiometric detection of reactive oxygen species in inflammatory cells. J Biophoton, 2018, 11: 201700015
113 Ju E, Liu Z, Du Y, et al. Heterogeneous assembled nanocomplexes for ratiometric detection of highly reactive oxygen species *in vitro* and *in vivo.* ACS Nano, 2014, 8: 6014–6023
114 Tanaka K, Miura T, Umezawa N, et al. Rational design of fluorescein-based fluorescence probes. Mechanism-based design of a maximum fluorescence probe for singlet oxygen. J Am Chem Soc, 2001, 123: 2530–2536
115 Shabat D, Hananya N, Green O, et al. A highly-efficient chemiluminescence probe for detection of singlet oxygen in living cells. Angew Chem Int Ed, 2017, 56: 1793–1796
116 Keng C L, Lin Y C, Tseng W L, et al. Design of peptide-based probes for the microscale detection of reactive oxygen species. Anal Chem, 2017, 89: 10883–10888
117 Yu M, Xie D, Phan K P, et al. A CoII complex for 19F MRI-based detection of reactive oxygen species. Chem Commun, 2016, 52: 13885–13888
118 Prow T W, Sundh D, Lutty G A. Nanoscale biosensor for detection of reactive oxygen species. Methods Mol Biol, 2013, 1028: 3–14 119 Chu W,
Chepetan A, Zhou D, et al. Development of a PET radiotracer for noninvasive imaging of the reactive oxygen species, superoxide, *in vivo.* Org Biomol Chem, 2014, 12: 4421–4431
120 Carroll V N, Truillet C, Shen B, et al. [11C]Ascorbic and [11C]dehydroascorbic acid, an endogenous redox pair for sensing reactive oxy-gen species using positron emission tomography. Chem Commun, 2016, 52: 4888–4890 121 Zhang W, Cai
Z, Li L, et al. Optimized and automated radiosynthesis of [18F]DHMT for translational imaging of reactive oxygen species with positron emission tomography. Molecules, 2016, 21: 1696–1706
122 Wilson A A, Sadovski O, Nobrega J N, et al. Evaluation of a novel radiotracer for positron emission tomography imaging of reactive oxygen species in the central nervous system. Nucl Med Biol, 2017, 53: 14–20
123 Hamblin M R. Strategies to potentiate immune response after photodynamic therapy. Int Soc Optic Photon, 2015, 932405 124
Wachowska M, Gabrysiak M, Muchowicz A, et al. 5-Aza-2ÿ-deoxycytidine potentiates antitumour immune response induced by photodynamic therapy. Eur J Cancer, 2014, 50: 1370–1381
125 Zhao H Y, Wang Y C, Qiu H X, et al. Photodynamic therapy and anti-tumor immunity (in Chinese). Chin J Laser Med Surg, 2014, (1): 34–38 [Zhao Hongyou, Wang Yucheng, Qiu Haixia, et al. Photodynamic therapy and anti-tumor immunity. Chinese Journal of Laser Medicine, 2014, (1): 34–38]
126 Garg A D, Agostinis P. ER stress, autophagy and immunogenic cell death in photodynamic therapy-induced anti-cancer immune responses. Photochem Photobiol Sci, 2014, 13: 474–487
127 Lee K B, Lee J S, Park J W, et al. Low energy proton beam induces tumor cell apoptosis through reactive oxygen species and activation of caspases. Exp Mol Med, 2008, 40: 118–129
128 Shahzidi S, Brech A, Sioud M, et al. Lamin A/C cleavage by caspase-6 activation is crucial for apoptotic induction by photodynamic therapy with hexaminolevulinate in human B-cell lymphoma cells. Cancer Lett, 2013, 339: 25–32
129 Pinghua T U, Huang Q, Yunsheng O U, et al. Aloe-emodin-mediated photodynamic therapy induces autophagy and apoptosis in human osteosarcoma cell line MG-63 through the ROS/JNK signaling pathway. Oncol Rep, 2016, 35: 3209–3215
130 Ito H, Matsui H. Mitochondrial reactive oxygen species and photodynamic therapy. Laser Therapy, 2016, 25: 193–199 131 Lamberti
M J, Pansa M F, Vera R E, et al. Transcriptional activation of HIF-1 by a ROS-ERK axis underlies the resistance to photodynamic therapy. PLoS One, 2017, 12: e0177801
132 Tan M, Zhu Y, Kovacev J, et al. Disruption of Sag/Rbx2/Roc2 induces radiosensitization by increasing ROS levels and blocking NF-ÿB activation in mouse embryonic stem cells. Free Radical Bio Med, 2010, 49: 976–983
133 Gozali M V, Yi F, Zhang J A, et al. Photodynamic therapy inhibit Fibroblast Growth Factor-10 induced keratinocyte differentiation and proliferation through ROS in Fibroblast Growth Factor Receptor-2b pathway. Sci Rep, 2016, 6: 27402 134 Han X B, Li H X,
Jiang Y Q, et al. Upconversion nanoparticle-mediated photodynamic therapy induces autophagy and cholesterol efflux of macrophage-derived foam cells via ROS generation. Cell Death Disease, 2017, 8: e2864

科学通报 Volume 63, Issue 18, June 2018

Summary for “Research progress of photodynamic reactive oxygen species”

Reactive oxygen species in photodynamic therapy

Xinpeng Jiang & Zhifei Dai*

*Department of Biomedical Engineering, College of Engineering, Peking University, Beijing 100871, China **
Corresponding author, E-mail: zhifei.dai@pku.edu.cn

Photosensitizer-mediated production of reactive oxygen species (ROS) plays a key role in photodynamic therapy (PDT). Reactive oxygen species mainly includes singlet oxygen, hydrogen peroxide, hydroxyl radical, superoxide anion radical and so on, among which singlet oxygen is the most important reactive oxygen species.

In this paper, we firstly introduce the basic property of reactive oxygen species, generation and elimination of endogenous reactive oxygen species and generation mechanism of exogenous reactive oxygen species based on light, oxygen and photosensitizer. Next, we focus on the photosensitizers used to generate reactive oxygen species, factors that affect the yield of reactive oxygen species, and methods to increase the reactive oxygen species con-centration at the tumor site. There are many factors that can affect the reactive oxygen species concentration at the tumor site, mainly among which are the singlet oxygen yield of the photosensitizer, the targeting of the photosensi-tizer, the oxygen concentration, and the illumination frequency. To achieve a good PDT effect, many photosensi-tizers or their nanoparticles with high singlet oxygen generation and good targeting ability are synthesized. Per-fluorocarbon is used to deliver oxygen to overcome oxygen deficiency. Upconversion nanoparticles and two-photon absorption are very useful to solve the problem of weak penetration of short-wavelength light. New PDT methods are also introduced in the text, such as PDT combined photothermal therapy or chemotherapy.

Then, we summarized various methods and technologies for reactive oxygen species detection, including direct detection of phosphorescence spectrophotometry, fluorescent probes and chemical probes for indirect detection, electron spin resonance, and positron emission tomography. The direct phosphorescence method mainly detects singlet oxygen based on the 1270 nm phosphorescence emission when singlet oxygen returns to the ground state.
The first method to enhance the 1270 nm phosphor signal is to use a NIR photomultiplier tube (PMT) or an InGaAs linear array in combination with scanning of the excitation laser beam, and the second one is based on the use of a NIR camera with a filter. Because the lifetime of singlet oxygen is very short, time resolution is especially im-portant. There are basically three main photon counting techniques: gated photon counting (GPC), multichannel scaling (MCS), and time-correlated single photon counting (TCSPC). In addition, singlet oxygen-sensitized delayed fluorescence (SOSDF) can also be used to detect singlet oxygen.

Various new types of probes can specifically detect different types of reactive oxygen species, for example, 9, 10-anthracenedipropionic acid and MitoSOX can be used to detect singlet oxygen and superoxide anion in living cells respectively. The fluorescent probe itself does not have fluorescence, but reacts with reactive oxygen species to form an inner oxide, and emits strong fluorescence under the excitation of a certain wavelength of light. The dif-ference of chemical probe is that it does not require light excitation because it can emit light spontaneously after reacted with reactive oxygen species. Electrons spin resonance (ESR) and positron emission tomography (PET) are also available to detect reactive oxygen species by using a probe.

Finally, we discussed the mechanism of reactive oxygen species killing tumor cells, mainly in the following three aspects: (1) direct toxicity to tumor cells and induce their necrosis, apoptosis or autophagy; (2) damage on the tumor capillary endothelial cells and destruction of the microvasculature; (3) activation of an acute inflammatory response in host defense mechanisms. The effect of reactive oxygen species on the immune system and the apop-totic pathway of tumor cells from genes, proteins to the cell level were described in detail.

photodynamic therapy, reactive oxygen species, singlet oxygen, photosensitizer, detection, mechanism

doi: 10.1360/N972018-00214